

Learning from failure: Damage and Failure of Masonry Structures, after the 2017 Lesvos Earthquake (Greece)

Georgios Vlachakis^{1*}, Evangelia Vlachaki², Paulo B. Lourenço¹

¹ISISE, Department of Civil Engineering, University of Minho, Guimarães, Portugal

²Independent researcher, Voreiou Ipeirou 9, 26500 Patras, Greece

*Correspondence to: Georgios Vlachakis, ISISE, Department of Civil Engineering, University of Minho, Campus de Azurém, Guimarães, 4800-058, Portugal; E-mail: giorgovlachaki@gmail.com

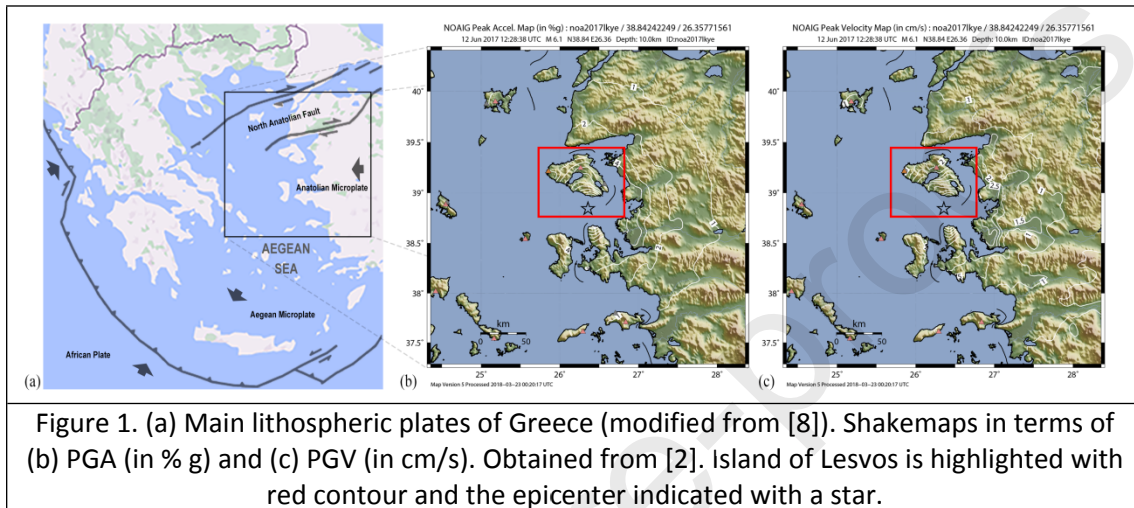
Abstract - On the 12th of June 2017 an earthquake of Mw=6.3 struck SSE of Lesvos Island, causing one human fatality and severe damage to the built environment. The traditional settlement of Vrissa was the most affected area, having masonry structures as the majority of its building stock. The objective of the present study is two-fold: to present the structural damage and failure patterns induced by the Lesvos earthquake to masonry structures; to highlight the causes and weaknesses that led to damage, or the factors that prevented it. Particular attention is paid to traditional construction techniques and architectural features that contributed to the seismic response of the structures, either having beneficial or detrimental effect. To this end, a field reconnaissance has been conducted and meaningful technical conclusions are drawn by the observations. Structural systems of both unreinforced and timber-reinforced masonry are inspected. Besides the identification of frequent cases of local, out-of-plane and in-plane mechanisms, combined global mechanisms are also pointed out. Finally, insight of the performance of past interventions is also given, assisting the challenging task of engineering practice.

Keywords: Seismic damage; Post-earthquake survey; Strengthening interventions; Performance; Traditional buildings

1. Introduction

On the 12th of June 2017, at 12:28 GMT, a shallow earthquake with magnitude Mw=6.3 struck SSE of Lesvos Island [1]. The epicenter of the seismic event, according to National Observatory of Athens (NOA) [2], had Latitude 38.84°N and Longitude 26.36°E, being approximately 15 km offshore of Lesvos island and with a depth of around 10 km. The seismic signal of the ground motion was instrumentally recorded only at distances of around 35 km at Mytilene in Lesvos island, and at Karaburun in Turkey, being both outside of the area of maximum damage [3]. The former station recorded PGA values of 0.024/0.070/0.044 [g] while the later 0.051/0.043/0.036 [g] for the NS, EW and vertical components, respectively. Subsequent studies estimated that the southern coast of Lesvos experienced PGAs of about 0.2 [g] [3] [4], or PGVs of about 0.3 m/s [5]. Figure 1 present the existing shakemaps available online by NOA [2]. It is understood that shakemaps provide only

38 approximate estimations of the seismic severity, as ground motion attenuation relations are
 39 employed. Moreover, it should be noted that the currently in-force Greek seismic code
 40 provides a PGA of 0.24 [g] for a return period of 475 years in the island, while more recent
 41 studies proposed even higher values [6]. The main seismic event was followed by over 500
 42 aftershocks in the subsequent four months [7], all concentrated in an area of about 30x10
 43 km² [4], expanding NW-SE of the mainshock's epicenter. Among these, 31 events had a
 44 magnitude greater than 3.5 Mw, with the largest one being 5.3, on the 17th of June at 17:50
 45 GMT.



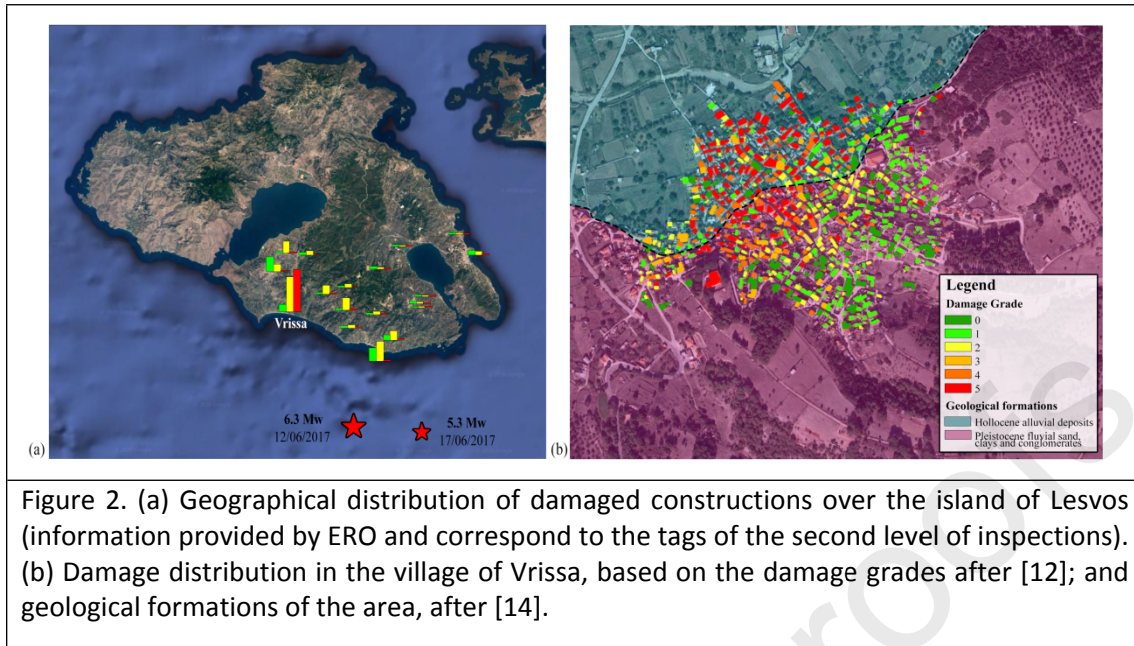
46

47 From a seismotectonic point of view, the 2017 Lesvos earthquake occurred at a seismically
 48 active region of the Aegean Region. The Aegean microplate is bounded by the Hellenic
 49 Trench to the south and by the western extension of the North Anatolian Fault to the north
 50 [1]. The northeastern Aegean is subjected to NE-SW dextral shearing transfer by the North
 51 Anatolian Fault and stretching due to slab rollback and gravitational spreading of the Aegean
 52 lithosphere [5]. More specifically, the Lesvos Island lies at the transition regime of the
 53 normal faulting of the western Anatolia and the strike-slip faulting in the Aegean. Three
 54 main fault systems have been recognized in the island [1], and the 2017 Lesvos earthquake
 55 mainshock and aftershocks ruptured the eastern segment of the Lesvos Basin fault [5]. The
 56 seismic sequence was associated with both normal and strike-slip faulting, along a NW-SE
 57 trending plane. More importantly, [1,5,7] among others, pointed out that the rupture
 58 propagated unilaterally to NW towards the south coast of Lesvos, where the most severe
 59 damage to the built environment was observed. This forward directivity characteristic
 60 appeared to have imposed near-fault effects to an area that has a relatively large distance
 61 from the epicenter, yet is just above the asperity with the major slip [5]. For more in-depth
 62 details of the seismological characteristics of the event, the reader is referred to [1,4,5,7,9].

63 In the same day, right after the seismic event, the Greek state emergency mechanism was
 64 mobilized and visited the island. More specifically, the Minister of Public Order, the
 65 Secretary-General of Civil Protection, the Secretary-General of Infrastructures, the President
 66 of Earthquake Planning and Protection Organization, directors of the Secretary-General of
 67 Civil Protection and of Earthquake Rehabilitation Organization (ERO), and members of the
 68 Special Unit for Disaster Mitigation were taken to the island by helicopters. The Lesvos

69 earthquake caused one human fatality and fifteen people were injured. Severe damage was
70 caused to the built environment, while all afflicted residents were relocated to temporary
71 housing. In the day after the earthquake, engineers of the ERO, assisted by local engineers,
72 started the first level of buildings' inspections (completed on the 25th of June). During this
73 process, 1.776 constructions were inspected, among which 937 were found as immediately
74 uninhabitable. The second level of inspections followed between the 26th of June to the 28th
75 of July, during which 1.650 constructions were inspected. Among them, 319 were tagged as
76 "unsafe for use", 867 as "temporary usage is not permitted" and 464 as "immediately
77 usable". The spatial distribution of the damaged constructions was concentrated at the
78 southwestern part of the island being mainly old masonry buildings, while some minor
79 damage was also reported in Mytilene, in Chios Island and at the facing coasts of Turkey
80 (Figure 2(a)). In fact, about 50% of the totally reported damaged constructions and 290 out
81 of the 319 severed damaged cases were reported in the traditional settlement of Vrissa. It
82 appeared that about 80% of the Vrissa's building stock was damaged (Figure 2(b)), becoming
83 the "epicenter" of the earthquake's destruction, with an estimated EMS-98 [10]
84 macroseismic intensity of IX [1]. Regarding the environmental effects, slope movements
85 were induced in some areas [3,4]; while a non-damaging tsunami of about 35 cm peak-to-
86 peak amplitude was reported at the Plomari port [11].

87 The fact that Vrissa settlement suffered by far most of the induced seismic damage caught
88 the attention of the scientific community [12]. Actually, it was reported as an "impact
89 paradox" due to the following two unexpected facts: 1) the settlement lies further inland
90 from the epicenter than other settlements with less damage (Figure 2(a)), and 2) the
91 northwestern part of the settlement concentrated the majority of the damage (Figure 2(b)),
92 despite having a uniform building stock. The available studies pointed out as the decisive
93 factors a synergy of seismic directivity and near fault effects, the geological alluvial deposits
94 of the northern part of the settlement, the presence of geotechnical unstable zones and the
95 vulnerable masonry constructions. More specifically, [5] highlighted that Vrissa is located at
96 a very short distance from the western edge of the fault and the slip patch at the same time,
97 while forward directivity was developed towards the settlement. Some structural
98 observations about the seismic motion directivity are provided in the Appendix. [3–5,12,13]
99 underlined that the northern part of the settlement lies over recent Holocene alluvial
100 deposits that amplified significantly the seismic motion (Figure 2(b)). [4,12] indicated that
101 the steep slopes of the western part of the settlement showed to be unstable and even
102 generating local landslides. The aforementioned remarks provide some justification of the
103 localization of damage in the Vrissa settlement, when compared to the surrounding area.
104 Nevertheless, the studies available in literature paid little attention to the structural aspects
105 of the building stock, as they were mainly limited to large-scale observations.



106 The objective of the present study is two-fold: to present the structural damage and failure
 107 patterns induced by the Lesbos earthquake to masonry structures; to highlight the causes
 108 and weaknesses that led to damage, or factors that prevented it. Throughout the process,
 109 particular attention is paid to traditional construction techniques and architectural features
 110 that contributed to the seismic response of those structures, either having beneficial or
 111 detrimental effect. Moreover, as earthquake engineering knowledge on masonry structures
 112 has been evolving rapidly over the last decades, actual seismic events provide a unique
 113 opportunity to learn from the response of real historical masonry constructions over a large
 114 scale (e.g.: [14–35]). Finally, an insight of the performance of past interventions is attempted,
 115 thus assisting the challenging task of engineering practice [37].

116 To this end, a field reconnaissance has been conducted by the first author at the area struck
 117 by the Lesbos earthquake. Given the safety concerns or limited access to private property,
 118 the majority of the buildings have been inspected from outside, with the inherent
 119 limitations. Moreover, almost no conclusions could be derived by completely collapsed
 120 buildings, restricting further the field reconnaissance. Nevertheless, observations and
 121 comments are accompanied by representative photos, while simplified sketches are
 122 provided in order to facilitate the interpretation and systematize the observations. All
 123 examples shown correspond to the settlement of Vrissa, unless otherwise stated, as this
 124 settlement witnessed most of the induced seismic damage for this event, as explained
 125 earlier.

126 The outline of the paper is as follows: Section 2 presents the construction typologies
 127 inspected, referring to the materials and the techniques used; Section 3 illustrates and
 128 classifies the observed damage and failure patterns; Section 4 reports about the
 129 performance of past interventions that have been recorded; and, finally, the conclusions of
 130 the study are summarized in Section 5.

131 **2. Construction Typologies**

132 The historical building stock of the settlement of Vrissa consists mainly of stone masonry
133 constructions, and less frequently of brick masonry constructions. The majority of these
134 were built at the second half of the 19th century and the beginning of the 20th century, as a
135 reconstruction process after a destructive earthquake that hit the area in 1845 [38] (pp. 659-
136 660). The residential buildings in most cases follow a rectangular in plan layout of about 4 x
137 10 m, and the height is up to 3 stories. The majority of the roofing and flooring systems are
138 made of timber, while the internal spaces are separated by internal walls, poorly connected
139 to the masonry façades. Timber-reinforced masonry buildings were also identified,
140 composing a small yet particular structural typology.

141 The following paragraphs provide an overview of the construction materials and techniques
142 that were identified in these constructions, highlighting structural aspects that played a
143 decisive role in the buildings' seismic response.

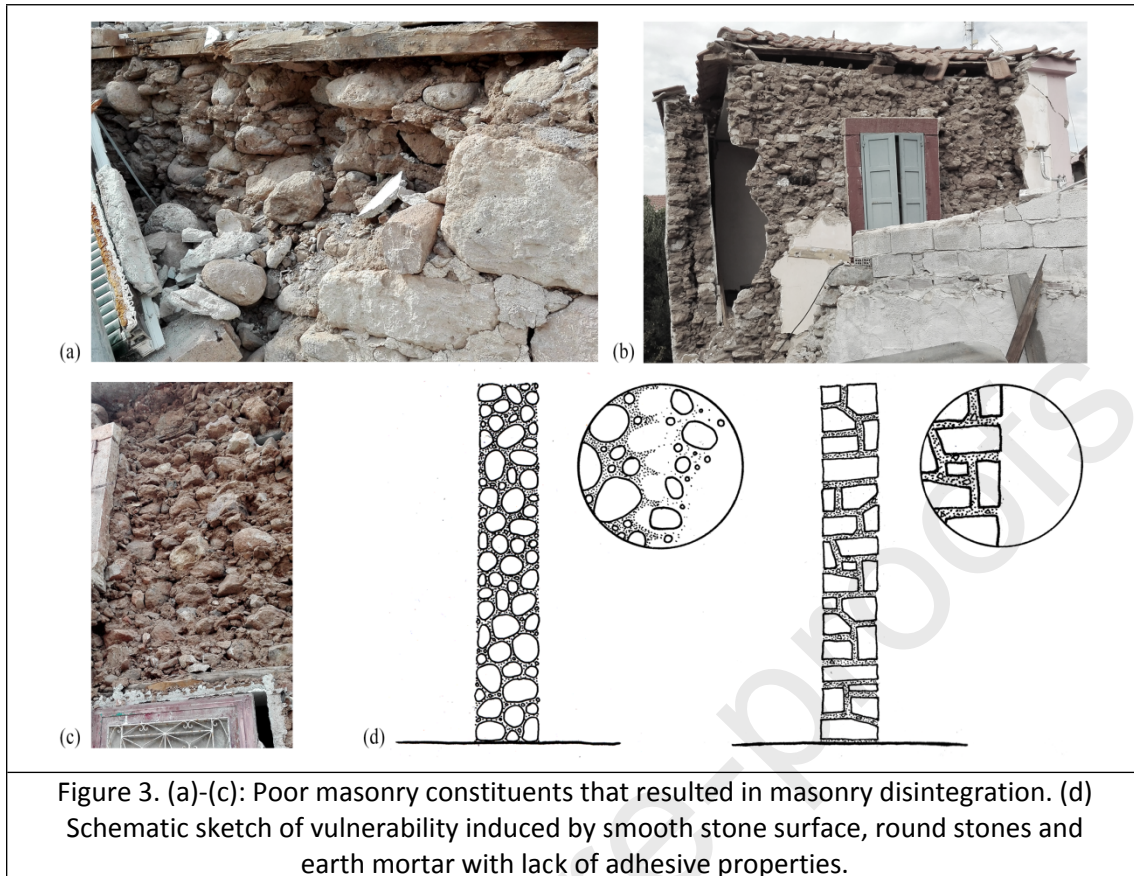
144 **2.1 Construction Materials**

145 In general, materials of poor quality were used in the masonry construction, resulting in
146 remarkably low seismic performance. Despite the good quality of ignimbrite stones
147 extracted at quarries in the surrounding area and the local brick manufactories, many of the
148 structural walls in the Vrissa settlement were built of relatively small river-side stones (i.e.
149 dimension smaller than 0.20 m), due to their abundant presence nearby and the ease of
150 collection. The smooth and round surface of such stones did not allow significant bond and
151 interlocking to be developed and structural walls disintegrated easily (Figure 3). Earth
152 mortar was mainly used in the masonry buildings, introducing further vulnerability. Such
153 mortar is characterized by low cohesive properties, low compressive strength and sensitivity
154 to water content (Figure 3). Lime and cement based mortars were also employed, but only
155 rarely, usually as subsequent repointing applications. A detailed investigation of the mortar,
156 as performed locally after the 2016 Central Italy [39] or after the 2010-2011 Christchurch
157 earthquakes [27], could provide a better insight of its characteristics and its role within the
158 masonry assemblage.

159 Material degradation contributed in worsening the performance of both masonry and
160 timber elements. The abandonment that the Greek countryside experienced in the last
161 decades resulted in substandard or lack of maintenance. Water ingress deteriorated both
162 the mortar and the timber elements.

163 Masonry built with rougher units or bricks was able to develop a more homogenized and
164 better response.

165

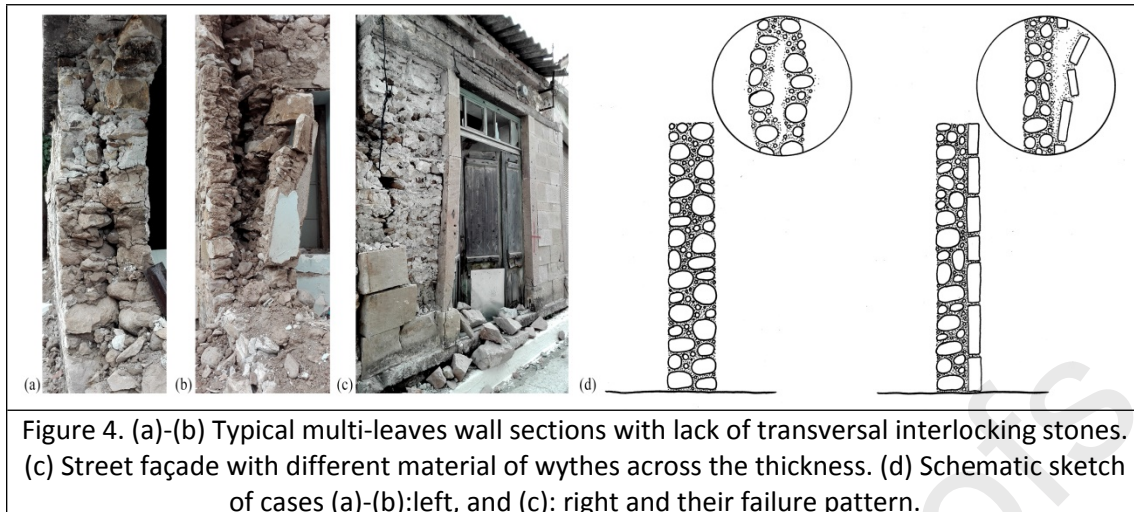


166 2.2 Construction Techniques

167 2.2.1 Unreinforced Masonry

168 UnReinforced Masonry (URM) buildings were constructed typically with two and three-leaf
 169 masonry walls with a thickness varying between 0.4 and 0.7 m. However, the lack of
 170 transversal interlocking stones (through stones, bond stones, tie stones or *diatono*) that
 171 could connect the external leaves, resulted in detachment and masonry delamination
 172 (Figure 3 (b), (c), Figure 4 (a), (b), (d)). This construction deficiency appeared to be crucial for
 173 the seismic response of the URM buildings, as it triggered or assisted many structural
 174 failures, as shown below.

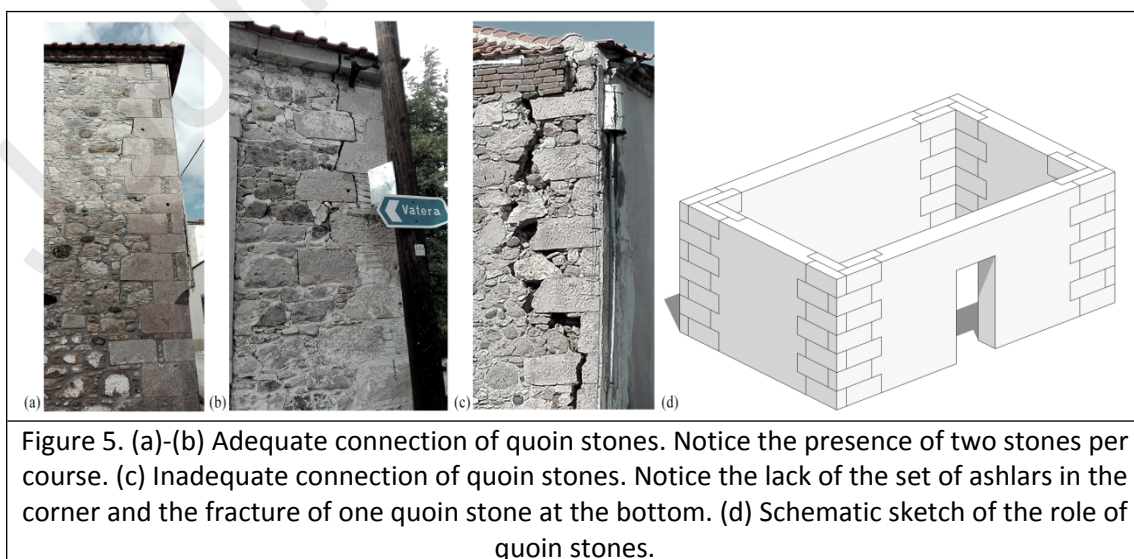
175 In some structures built at the central part of the settlement, a different kind of building
 176 material was used between the parallel leaves. Perfectly cut stones were employed for the
 177 outer leaf of the façade in order to demonstrate wealth and solidity, while rubble stones
 178 were used for the rest of the section (Figure 4 (c), (d)). Once again, no mechanical
 179 connection between the leaves was ensured, while the different stiffness of the masonry
 180 across the section increased its vulnerability.



181

182 The corners of URM buildings were usually constructed with quoin-stones. Well-shaped and
 183 in most cases, being made with more than a single stone in the course, quoins helped the
 184 connection of transversal walls, preventing local or global failures (Figure 5 (a), (b), (d)), as
 185 shown below. Still, quoins were often insufficient to prevent the development of corner
 186 cracks, especially when an additional set of ashlar stones was poorly constructed or missing
 187 (Figure 5 (c)). The use of ashlar stones was also adopted for the stones in the frames around
 188 building openings. Often, monolithic squared stones were used for posts and lintels around
 189 the openings, as a local architectural feature. The lack of proper interlocking of these
 190 elements with the rest of the masonry, leads to the assumption that these are decorative,
 191 non-structural elements.

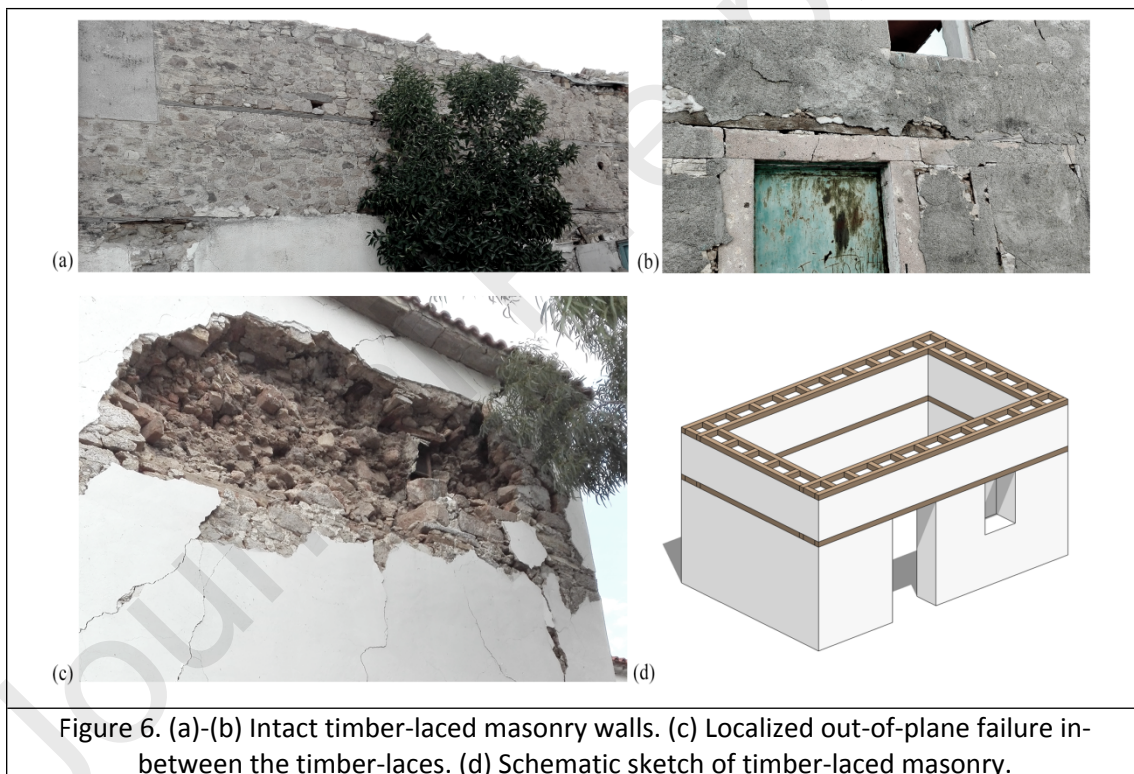
192 Tie rods, commonly used in the Mediterranean region, were observed on just three buildings
 193 of the settlement (Figure 9 (c)). Despite the fact that the benefits of this technique (see e.g.
 194 [40] and references therein) were well understood in the past, its extended use was
 195 probably hampered in the area due to the difficulty in finding metal ties on the island and
 196 socioeconomic reasons.



197 2.2.2 *Timber-reinforced Masonry*

198 The use of timber elements has been recorded throughout the history of structural systems
 199 developed in Greece, for almost 5000 years, as a technique to improve the seismic response
 200 of structures. A chronological and regional overview of the vast variety of timber-reinforced
 201 masonry types can be found in [41]. Such structural solutions were observed also in the
 202 settlement of Vrissa, in the forms of: *i) timber-laced masonry*, and *ii) timber-frame masonry*.

203 *Timber-laced masonry* consists of timber ring beams placed at regular spacing across the
 204 height and as a pair across the thickness of the walls (Figure 6). Such a technique, as
 205 described in [41–44] and references therein, improves the seismic performance of the
 206 building in its inelastic range, by providing horizontal slip planes, dissipating energy and
 207 enhancing the masonry In-Plane (IP) and Out-Of-Plane (OOP) strength by confining portions
 208 of the walls. In addition, this technique enhances the connection between transversal walls
 209 and helps to tie the leaves of a wall together and avoid disintegration. During the
 210 reconnaissance campaign, the damage that was observed in timber-laced masonry
 211 structures was limited in-between the ring-beams across the height, demonstrating the
 212 adequacy of the system (Figure 6 (c)).



213

214 *Timber-frame masonry* (local name “*friggi*” [45]) consists of a composite structural system
 215 of a timber-frame with vertical posts, horizontal beams and diagonal bracing elements,
 216 together with masonry walls having one leaf as infill of the frame and the other as external
 217 cover of the frame (Figure 7). In most cases, the timber-frame system was observed to exist
 218 only on the upper floors, while resting on horizontal timber-laces at the crest of the masonry
 219 ground floor. In fact, the presence of the internal timber-frame seems to exclude the
 220 construction of timber-laces at the same areas. It appears that the two systems were not

221 used complementary, but each one was considered sufficient by the local masons; a remark
 222 noted also by [46]. Moreover, special L-shaped corner elements were recognized at the
 223 timber connections in several buildings, providing increased stiffness and energy dissipation
 224 to the frame (Figure 7 (b), (d)). Similar structural systems in the world have been observed
 225 with a remarkably low vulnerability to earthquake actions; e.g. in [23,46,47]. During the field
 226 reconnaissance, only one total-collapse of such a structure was observed, probably due to
 227 other deficiencies that could not be recognized from the debris. More specifically, damage
 228 was mainly localized in the outer unreinforced leaf of the masonry walls resulting in OOP
 229 failures, while the timber-frame could stand the whole seismic event (Figure 7 (a), (b)). This
 230 structural redundancy prevented both inward collapses of the masonry walls and complete
 231 collapse of the roof system, thus protecting the buildings' inhabitants. Yet, one could argue
 232 that such OOP failures could have been prevented if the timber-frame was also confining the
 233 outer leaf with timber-laces at regular distances. Furthermore, it should be noted that the
 234 damage was much more extensive in cases with deficiencies, such as the irregular
 235 configuration of the braces, the lack of continuity of the timber-frame at the ground floor,
 236 the presence of poor connections or the level of degradation of the timber (Figure 7 (c)).



Figure 7. (a)-(b) Localized out-of-plane collapse of external unreinforced leaf. Notice the L-shaped corner elements in (b). (c) Extensive damage due to timber deterioration and poor connections. Notice the lack of the timber-frame system at the ground floor. (d) Schematic sketch of timber-frame masonry.

237 3. Damage and Failure Patterns

238 The earthquake-induced damage and failure patterns are described next, following a
 239 qualitative distinction of two limit states commonly used in earthquake engineering. In order
 240 to facilitate reading and to establish meaningful conclusions, the presentation is done
 241 according to a systematic classification of mechanisms. The description starts with local
 242 mechanisms, followed by the critical OOP mechanisms and the desirable IP mechanisms.
 243 Subsequently, three types of combined IP and OOP mechanisms are presented. Finally, the
 244 failure mechanisms of non-structural components are highlighted.

245 3.1 Local Mechanisms

246 Since masonry is non-homogeneous and non-monolithic, with negligible tensile strength and
 247 high mass, local failure mechanisms often occur prematurely during earthquake events.
 248 Whenever these local mechanisms are not prevented through proper construction details
 249 and structural connections; they may be activated even under small seismic input and lead
 250 to partial collapse, which provides very high structural vulnerability and a form of non-
 251 acceptable failure.

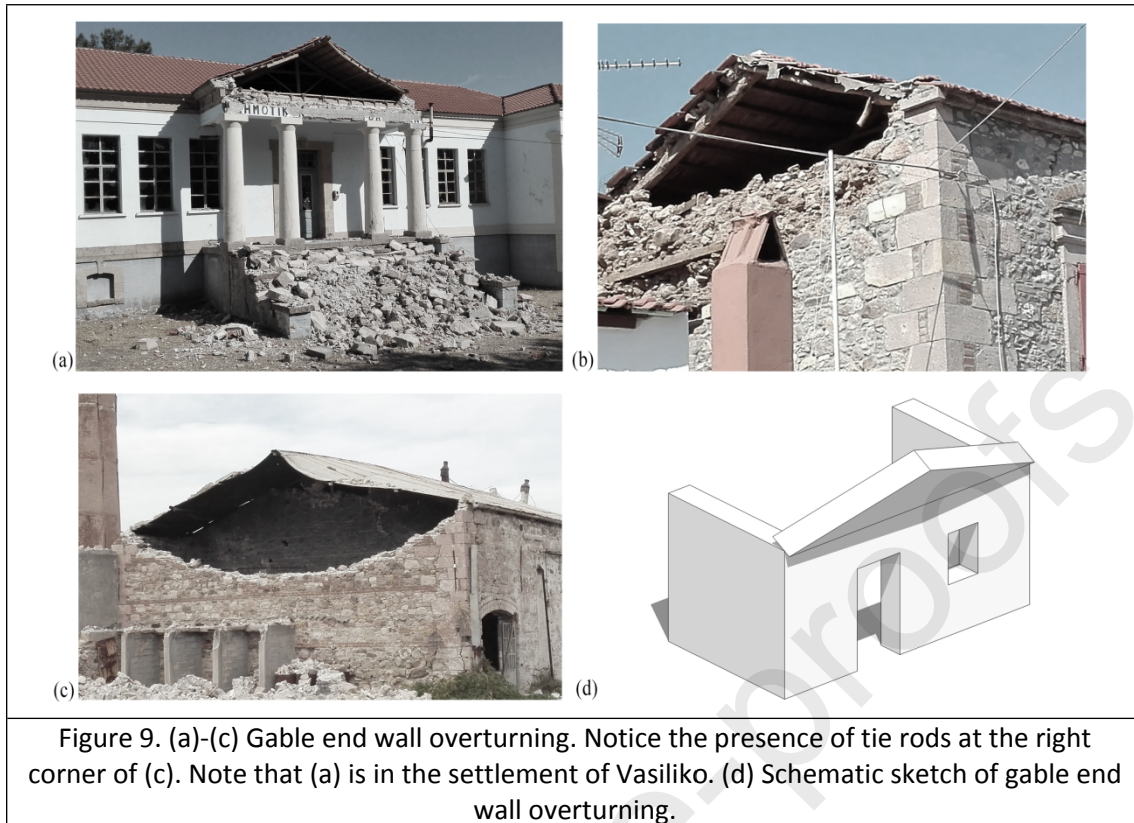
252 Disintegration of masonry can be considered a local mechanism in essence. In literature, it is
 253 also referred to as the “zero” mechanism [26], appearing when a masonry portion is unable
 254 to counteract almost any horizontal action and crumbles into pieces. Many cases of
 255 disintegration were identified during the reconnaissance, mainly as delamination of the
 256 external leaf (Figure 3, Figure 4 and Figure 8). The main factors that triggered such
 257 mechanisms are related to the low quality of the materials, the lack of interlocking stones of
 258 the different leaves or the lack of connection of the leaves with timber-laces.



Figure 8. (a)-(d) Local failures of the external leaf due to wall disintegration.

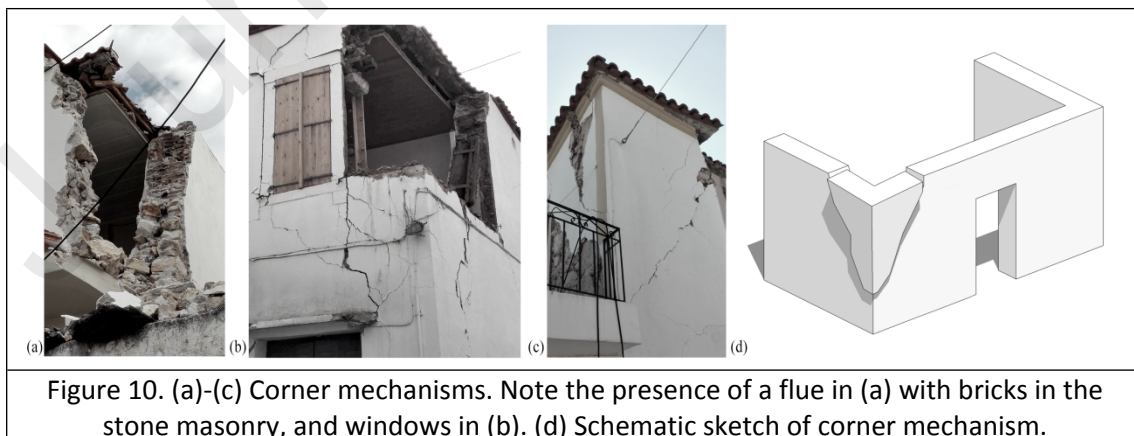
259

260 Overturning of gable end walls is a frequently occurring local mechanism. The notable
 261 vulnerability of this part of the constructions is attributed mainly to the inadequate
 262 connection with the roofing system and the lack of overburden weight (as the roof rafters
 263 are usually laid on the transversal walls), together with the amplified accelerations at the
 264 gable's height. Several collapses of gable walls were observed during the reconnaissance
 265 (Figure 9). Among them, it is worth to mention the gable wall collapse of the elementary
 266 school of Vasiliko, a settlement of around 7km further inland from Vrissa which suffered
 267 almost no damage. This further highlights the vulnerability of the mechanism (Figure 9 (a)).



268

269 Another common local mechanism concerns the top part corners of buildings (Figure 10).
 270 This mechanism originates from the lack of a diaphragm; often in presence of adequate
 271 connections by the quoin-stones, preventing façade detachment and overturning [48,49]. As
 272 a result, a combination of IP rocking-sliding and OOP flexural failure occur, forming wedge
 273 type diagonal cracks. Furthermore, the vulnerability of this mechanism is increased by the
 274 presence of a thrusting roof, and neighboring openings or flues at the transversal walls.
 275 Finally, it should be noted that the occurrence of such mechanism reduces significantly the
 276 capacity of the connecting transversal façades, as they lose a vital transversal support.



277

278 Local failures were also observed in areas of fireplaces' flues (Figure 11). The usual
 279 configuration of embedding the fireplace's flue within masonry induces a local section

280 reduction at the wall that makes it much more vulnerable. It is noted that the material
281 degradation caused by the fire and cycles of thermal expansion / contraction further reduces
282 the capacity. Moreover, the vertical discontinuity introduced by the section reduction, could
283 trigger other mechanisms as well.

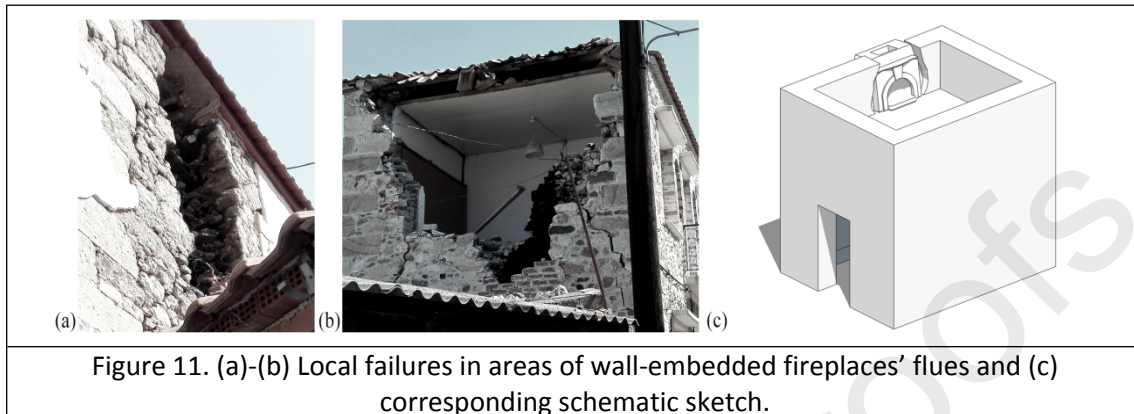


Figure 11. (a)-(b) Local failures in areas of wall-embedded fireplaces' flues and (c) corresponding schematic sketch.

284 3.2 Out-of-plane Mechanisms

285 In the absence of a “box like behavior” of structures, i.e. a global or integral behavior of the
286 building induced by horizontal diaphragms that connect the structural in a unified response,
287 the inertial forces of the walls perpendicular to the seismic action give rise to OOP bending.
288 The capacity of masonry structures under such action is particularly low, and led to most
289 collapses during the earthquake in Lesvos, alike similar events.

290 Long walls or walls with insufficient transversal support suffer vertical, one-way bending. In
291 particular, the top part of the façades, usually inadequately connected with the roof,
292 behaves as a cantilever about their base or the underneath floor level (rocking type of
293 failure). Similarly, walls with adequately connected transversal walls experience two-way
294 bending, characterized by larger capacity in comparison with the former. Figure 12 depicts
295 typical OOP collapses.



Figure 12. (a)-(d) Typical out-of-plane failures under one-way and two-way bending. Note that (d) shows the elementary school of Vrissa settlement.

296

297 The typical plan layout of the constructions in the area contributed to the development of
 298 one-way OOP bending. Since the internal walls were not connected with the masonry walls,
 299 the resulting unconstrained length of the façades (around 10 m) was too large. Several cases
 300 were observed in which one intermediate wall was shared between two structural units; yet
 301 one of them was just resting on the common wall, lacking connection. Such configuration
 302 usually appears when the two units were built at different periods, and the latter unit
 303 increased the internal space by utilizing the existing wall. The seismic vulnerability of such
 304 configuration is clear from a structural point of view, as the transversal façade of the latter
 305 unit lacks a lateral support (Figure 13). A traditional solution in such cases is the insertion of
 306 protruding (or “toothing”) stones to ensure interlocking, although this was not observed in
 307 the field reconnaissance.



Figure 13. (a)-(c) Out-of-plane failures of façades with unconnected walls juxtaposed, with no interlocking, and (d) corresponding schematic sketch.

308

309 Furthermore, the presence of transversal walls is not a *de facto* guarantee of their
 310 effectiveness. An adequate connection capacity is required in order to distribute the inertia
 311 forces of the OOP façade to the in-plane walls, typically ensured by quoin-stones (Figure 5),
 312 timber-laces (Figure 6) or tie rods (Figure 9 (c)). The importance of the corner connections
 313 was appreciated by local masons, as it can be recognized by observing the existing
 314 construction details. However, in several buildings the quoins were not sufficient, especially
 315 when the second set of stones in a course was poorly constructed or missing, making a short
 316 connection. Moreover, the presence of openings at the proximity of the corners appeared to
 317 reduce the strength of the corner connections (Figure 14). In the same context of lateral
 318 support, the architectural feature of buildings' entrance with a recess door acted beneficially
 319 for the façades, introducing flanges (Figure 15). A representative example is shown in (Figure
 320 15 (a)), where the transversal walls of the entrance recess suffered IP damage, indicating
 321 their role of supporting the main façade. Nevertheless, this attribute was only effective for
 322 the ground floor.



Figure 14. (a)-(d) Weak connection of transversal walls, due to the presence of openings at the corner proximity.

323

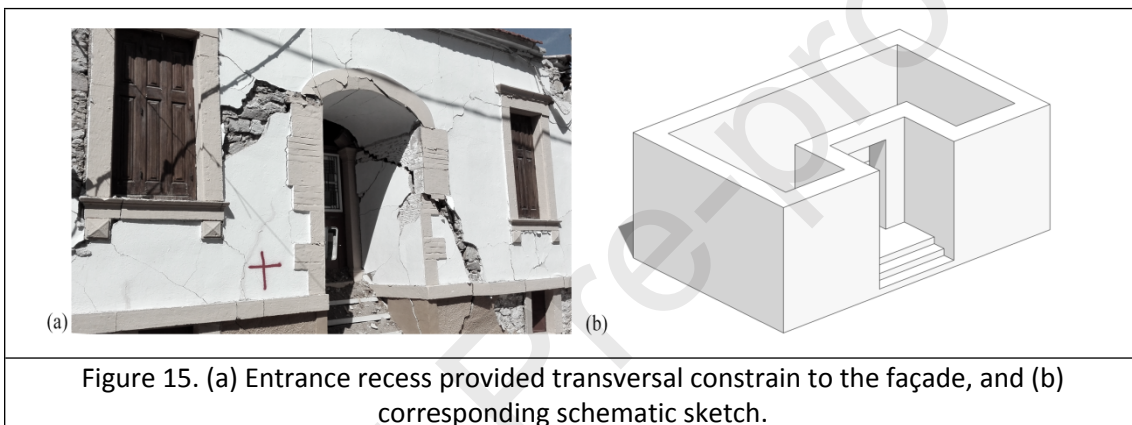


Figure 15. (a) Entrance recess provided transversal constrain to the façade, and (b) corresponding schematic sketch.

324

325 The vulnerability of the masonry walls is also governed by the slenderness, with more
 326 damage for walls with higher interstory height. Due to the acceleration amplification across
 327 the height and the lower overburden weight, many OOP collapses of top parts of slender
 328 walls were observed (Figure 12). A representative example of the aforementioned
 329 characteristics can be recognized in slender downhill side façades (Figure 16).

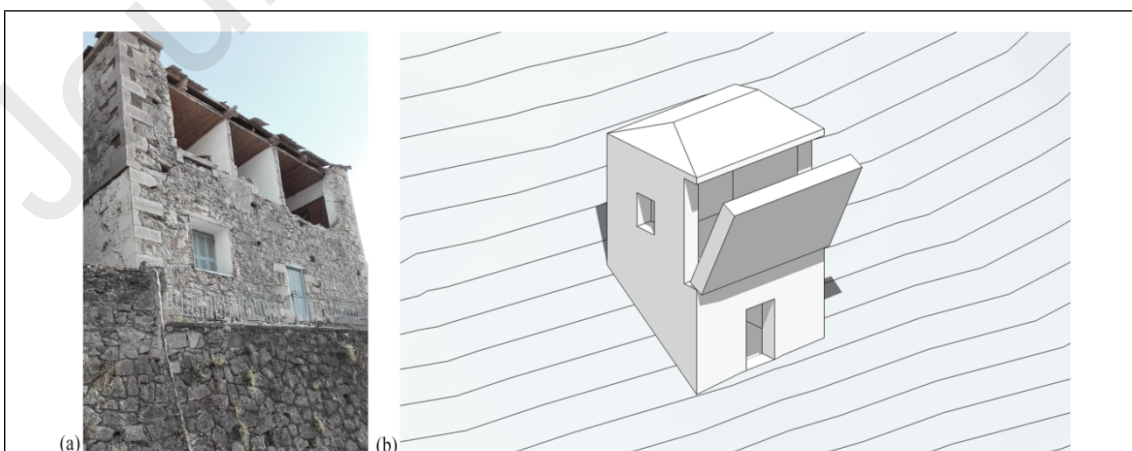


Figure 16. (a) Out-of-plane collapse of downhill side façade, and (b) corresponding schematic sketch.

330 It is well known that horizontal elements can contribute to prevent OOP failures by
 331 constraining the façade; yet insufficient connections with the masonry walls were observed
 332 for these elements. With the exception of the cases with timber laces, the timber roofs and
 333 floors were simply resting on the masonry walls, thus possessing only limited frictional
 334 horizontal capacity, which was inadequate to cope with OOP inertia forces. Moreover, the
 335 floors were spanning only in one (main) direction, supported by two parallel walls.
 336 Therefore, transversal walls were not connected by the horizontal systems, a necessary
 337 condition for diaphragmatic action. A few cases of localized damage due to thrust action of
 338 the roof were observed (Figure 17). It should be noted that timber sill plates were employed
 339 at the end of the timber beams, in order to distribute smoothly the gravity forces, thus
 340 avoiding local wall failures (Figure 12 (a)-(c)).



Figure 17. (a)-(b) Localized damage due to roof-thrust action.

341

342 Plan irregularities led also to OOP mechanisms. Figure 18 (a) shows a protrusion of a building
 343 that concentrated severe damage due to torsional phenomena taking place. Figure 18 (b)-(c)
 344 displays a case of complete collapse of the first floor. By looking to its condition before the
 345 seismic event, it appears that the owners demolished the corner of the building at the first
 346 floor in order to create a balcony. This eliminated any connection of the transversal walls
 347 and introduced a plan irregularity, certainly contributing to collapse.

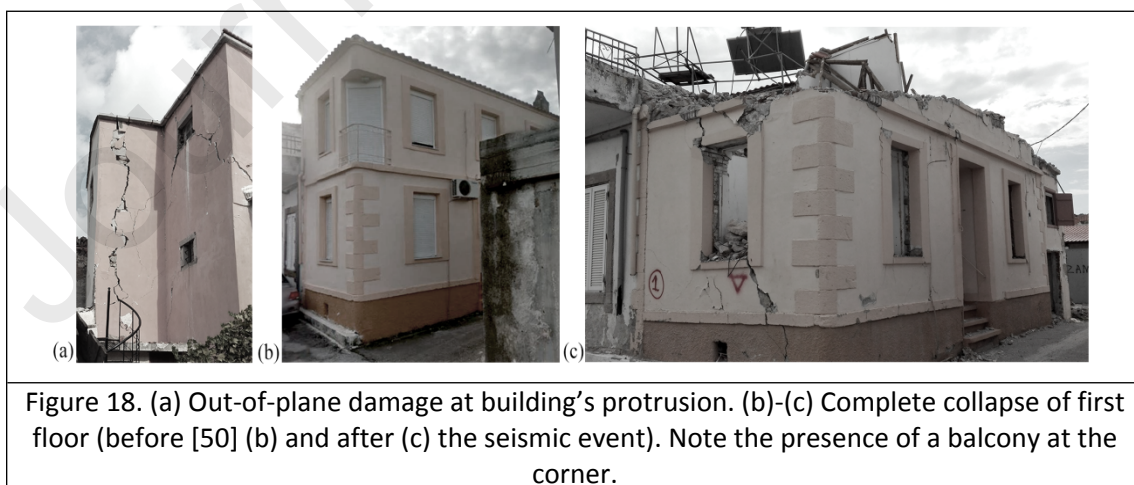


Figure 18. (a) Out-of-plane damage at building's protrusion. (b)-(c) Complete collapse of first floor (before [50] (b) and after (c) the seismic event). Note the presence of a balcony at the corner.

348 3.3 In-plane Mechanisms

349 The IP response of masonry structures is in general preferred, as it utilizes the largest
 350 capacity of the walls, dissipates significant energy and provides less brittle collapses. In fact,

351 in such cases damage tends to be prevented, unless the in-plane area of masonry walls is too
352 low or the openings are badly positioned. The mobilization of IP behavior requires the
353 prevention of local and OOP mechanisms, usually with the help of a diaphragm or densely
354 spaced transversal walls. During the field reconnaissance, typical IP damage patterns were
355 observed and are described here.

356 In most buildings where the plan and elevation regularity is respected, damage is distributed
357 in the so-called masonry members, i.e. the piers and spandrels. On the other hand, buildings
358 with irregular configuration exhibit damage concentration at the weakest areas (Figure 19).

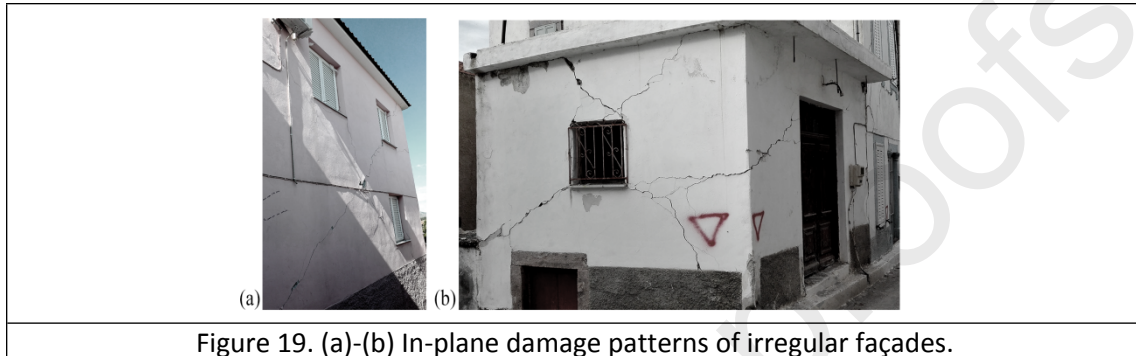


Figure 19. (a)-(b) In-plane damage patterns of irregular façades.

359

360 Shear damage, usually exhibited by squat walls, appears mostly as diagonal tension with
361 joint sliding in case of good quality masonry. The diagonal tensile mechanism occurs when
362 the principal tensile stress at the center of the member reach its tensile capacity. This mode
363 is characterized by larger brittleness, while it develops as a pair of diagonal X cracks over the
364 member, in the case of rubble masonry with almost straight cracks. The joint sliding
365 mechanism takes place when the frictional capacity of the member is exceeded. This mode
366 shows a ductile behavior, and appears either as a pair of X stepwise cracks or as horizontal
367 crack over the member (the latter more uncommon). Flexural damage affects mainly slender
368 members. It appears at the member's end sections (e.g. top or bottom for piers) either as
369 tensile cracks or as toe-crushing. This damage mode exhibits large displacement capacity,
370 until toe crushing occurs. Finally, any combination of the aforementioned modes is
371 commonly observed, especially after cyclic loading reversals. Figure 20 illustrates
372 representative cases of the aforementioned IP damage patterns.

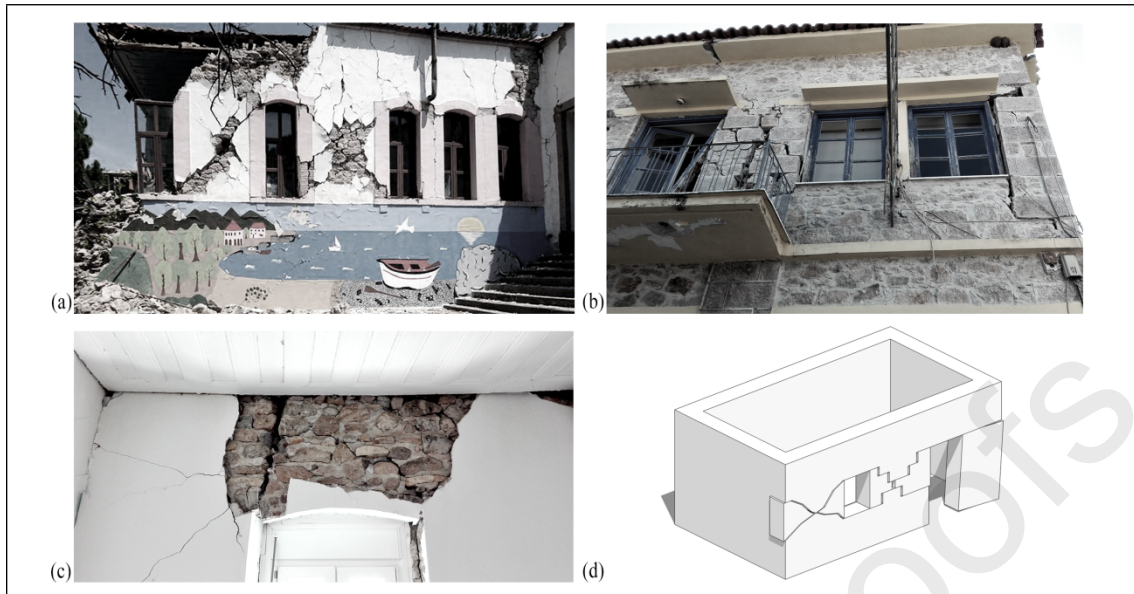


Figure 20. Typical in-plane damage pattern of: diagonal tension (two piers at the left of (a)), joint sliding (left pier of (b) and spandrel of (c)), flexural (right piers of (a), right pier of (b) and spandrel of (c)). Note that (a) shows the side façade of the elementary school of Vrissa settlement. (d) Schematic sketch of in-plane damage patterns.

373

374 As expected, URM structures that experienced IP damage were mostly cases with a
 375 Reinforced Concrete (RC) slab (Figure 19 (a)-(b), Figure 20 (b), Figure 21). By its inherent
 376 stiffness, the slab acts as a diaphragm and thus prevents OOP mechanisms. Nevertheless, it
 377 should not be disregarded that RC slabs possess significant weight and therefore increases
 378 also, moderately, the seismic demand (in masonry buildings most of the weight remains in
 379 the walls). Figure 21 illustrates a building with particularly large mass due to the RC slabs
 380 that even extend to balconies, with severe IP damage in the ground floor.



Figure 21. Severe in-plane shear damage at the ground floor of a building with large mass in the reinforced concrete floor slabs.

381 **3.4 Combined In-plane and Out-of-plane Mechanisms**

382 Except the distinct occurrence of IP or OOP damage mechanisms, three combined IP and
 383 OOP mechanisms were observed and recorded during the field reconnaissance. It is of
 384 interest to note that combined mechanisms are poorly studied in literature, especially in
 385 terms of available methodologies for assessment and design.

386 The most frequent combined mechanism was the interaction, leading to both: 1) vertical
 387 cracks at the end sections of the spandrels that derive from the IP flexure of the spandrel
 388 and the OOP response of the façade; 2) diagonal cracks at the lower corners of the openings
 389 propagating towards the corners of the structure, that arise by the IP shear damage and the
 390 OOP behavior of the façade (Figure 22). An additional characteristic of this mechanism is
 391 that in most cases it appears mirrored in the transversal façades. The corner mechanism,
 392 mentioned in Section 3.1, is a local manifestation of this mechanism.



Figure 22. (a)-(c) In-plane and out-of-plane interaction mechanism, and (d) corresponding schematic sketch.

393

394 Observed only in a few cases, another identified combined mechanism was the wedge
 395 biaxial failure. This appears as a second order mechanism of the previous combined, when
 396 the top part of the construction is restrained. Under this condition, a wedge (usually the
 397 corner of the building) is highly stressed by the biaxial actions up to its capacity, resulting in
 398 a bursting collapse (Figure 23). In case of corners, the failure surface forms a rhombus that
 399 expands over the two transversal walls. In addition, this mechanism was also observed at
 400 the recess corner of a plan-irregular structure, where high biaxial stresses concentrated

401 (Figure 23 (c)). It may be worth mentioning that cut corners, a commonly observed
402 functional detail for street widening (e.g. see the bottom part of the corner at Figure 5 (a)),
403 significantly reduce the capacity of this mechanism.



Figure 23. (a)-(c) In-plane and out-of-plane biaxial wedge mechanism, and (d) corresponding schematic sketch.

404

405 Another combined mechanism observed was the OOP collapse of a previously IP damaged
406 wall. This mechanism refers to the strength degradation induced by IP damage to a portion
407 of the masonry wall, which may then be isolated and overturned by OOP actions (Figure 24).
408 The reverse situation was not observed in the field reconnaissance, but it should not be
409 excluded.



Figure 24. (a)-(c) Out-of-plane collapse of in-plane damaged members, and (d) corresponding schematic sketch.

410 3.5 Non-structural Components

411 Damage or failure of non-structural components is often associated to significant economic
 412 losses, loss of functionality and potential threats to life safety [51]. Therefore, the damage
 413 induced to non-structural components was recorded and is presented herein.

414 Similarly with previous earthquake reconnaissance, collapses were observed in retaining and
 415 veneer walls (Figure 25 (a)), pillars (Figure 25 (b)), chimney tops (Figure 25 (c)), roof tiles
 416 (Figure 25 (d)) and infilled window openings. Yet the most crucial and widespread of non-
 417 structural failures appeared to be the monolithic stones used for posts and lintels of the
 418 openings (Figure 25 (e), (f)). As discussed in Section 2.2.1, this local architectural feature of
 419 the settlement did not possess any connection or interlocking with the rest of masonry and
 420 thus detached easily. More importantly, collapse could undoubtedly lead to fatalities, as
 421 massive stones collapsed at the entrance of the buildings and in the streets during the
 422 seismic event.



423 **4. Interventions**

424 It is usual that old structures undergo some kind of intervention during their lifetime. Such
 425 actions may alter, or fail to alter, the seismic response of the structure. The existing
 426 knowledge of the effect that interventions have on masonry structures is generally limited;
 427 especially when referring to real applications, where the controlled conditions and
 428 assumptions of the laboratory testing do not necessarily apply. This stresses the need to
 429 assess the effectiveness (or vulnerability) of interventions by studying their performance in
 430 actual seismic events.

431 A remarkable example of the lessons learnt after seismic events is Italy. Destructive
 432 earthquakes that hit Italy in the 1970's and 1980's led to the adoption of strengthening
 433 measures in the national codes as well as actual applications to reduce the seismic
 434 vulnerability of masonry structures. However, the effectiveness and compatibility of many of
 435 the adopted techniques was questioned deeply after the seismic events that followed in the
 436 next decades, as their performance was tested [16,19,25,52–54]. Thus, the national codes
 437 were changed, limiting and even banning some of the techniques adopted in the past.
 438 Nevertheless, studies of more recent seismic events highlighted that strengthened
 439 structures according to the past seismic codes performed better than non-strengthened
 440 structures, which is in disagreement with the previous outcomes [21,37].

441 Two aspects become clear from the past observations: 1) documenting the performance of
442 previous interventions after a seismic event can highlight their benefits and reveal their
443 shortcomings; and 2) the choice and application of intervention measurements for masonry
444 structures is a nontrivial task in engineering that should be carried out with caution. In fact,
445 as [16] stated, “*there are not bad techniques but only inappropriate and poor applications*
446 *due to lack of knowledge and of skillness [sic]*”. Nevertheless, well-considered and well-
447 applied interventions have persistently shown an enhancement in the seismic performance,
448 being encouraging and promising for future developments [21,27,37,55].

449 Keeping in mind the above, the following paragraphs attempt to shed light in the
450 performance of observed interventions, while drawing meaningful conclusions. A basic
451 distinction is pursued, based on the scope of the interventions: a) those that aim to restore,
452 strengthen or upgrade the structural unit; and b) those that aim to change or redefine the
453 use of the structural unit, causing structural alterations.

454 **4.1 Performance of Strengthening Techniques**

455 Firstly, interventions that have the explicit intention of improving the structural behavior are
456 studied. Three categories of interventions are considered according to the purpose:

- 457 1. To ensure the integrity and solidity of the masonry assemblage
- 458 2. To ensure the connections of structural elements
- 459 3. To increase the capacity or stiffness of structural elements

460 This categorization may be understood also as a strengthening hierarchy (or prioritization).
461 In principle, the integrity of masonry comes before adequate connections of structural
462 elements, which in turn come before enhancing capacity of structural elements for better
463 seismic performance. In other words, interventions that increase the capacity of structural
464 elements would be less relevant, if the different elements are not adequately connected;
465 while, the assurance of structural connections would not be fruitful, if the masonry
466 disintegrates. This framework can assist in interpreting the observed performance of
467 previous interventions.

468 Several cases were identified in which a RC beam was introduced at the top of masonry
469 walls (Figure 26 (a), (b)). This strengthening technique falls in the second category and could
470 be beneficial, as it connects and ties the transversal walls (and may add overburden weight),
471 thus reducing the OOP vulnerability of the façades. Nevertheless, local or even global
472 collapses were observed in such cases, with the masonry walls disintegrating (“zero”
473 mechanism). Given the extremely poor quality of masonry, the integrity of the underlying
474 walls was not ensured in order for the enhanced connections to be beneficial. In addition,
475 one could argue about the damage introduced by adding the beam or the subsequent
476 incompatibility of deformation, and about an increase in the demand of the poor masonry
477 walls, due to the added mass of the RC elements, or the destabilizing OOP moments that
478 arise by an eccentric interaction at imposed deformations (p - δ effects) [56].

479 A similar response was seen in cases that a RC slab had substituted the roofing system
480 (Figure 26 (c)). The addition of a rigid diaphragm was not able to improve the seismic

481 response of the underlying poor masonry. Had the masonry's integrity been ensured, the
 482 diaphragm could be beneficial.



Figure 26. (a) Building strengthened with RC beam, (b) wall strengthened with RC beam and (c) wall strengthened with RC slab, all collapsed due to the poor quality of masonry. (d) Schematic sketch of failure of poor masonry strengthened with RC elements.

483

484 Finally, a few cases of RC jacketing were observed. This strengthening technique falls in the
 485 third category, as it intends to increase the capacity and stiffness of the masonry walls, both
 486 for IP and OOP actions. However, as the application was once more over a poor masonry
 487 substrate, failure and collapse were found (Figure 27). At this point it is interesting to note
 488 that if a proper detailing is performed, with applications on both sides of the walls and well-
 489 designed anchors, RC jacketing could act beneficially also for the integrity of the masonry,
 490 i.e. the first category. Nevertheless, very deficient applications of this strengthening
 491 technique were found (Figure 27 (c)), as application was only on the internal surface and
 492 using sparse anchors. The images illustrate clearly that it was masonry that failed rather than
 493 the reinforcement, corroborating the need of prioritization of strengthening interventions.

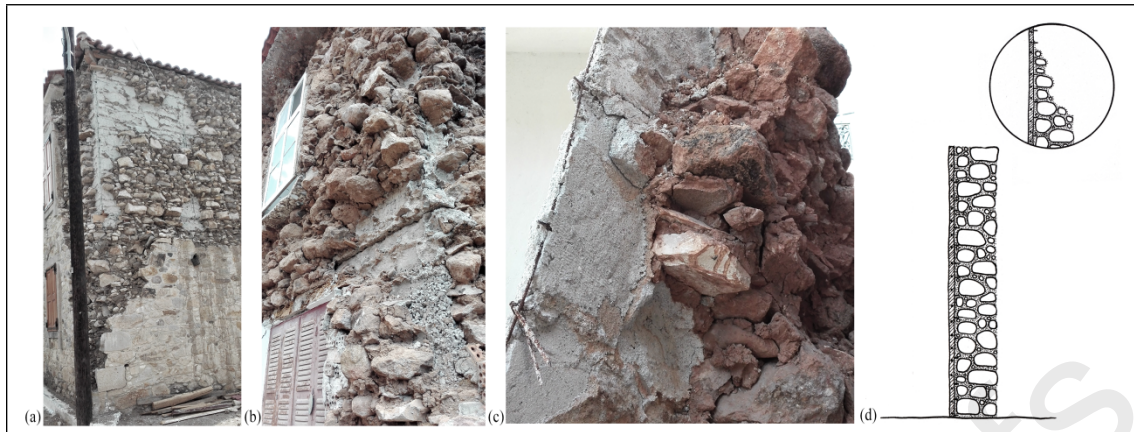
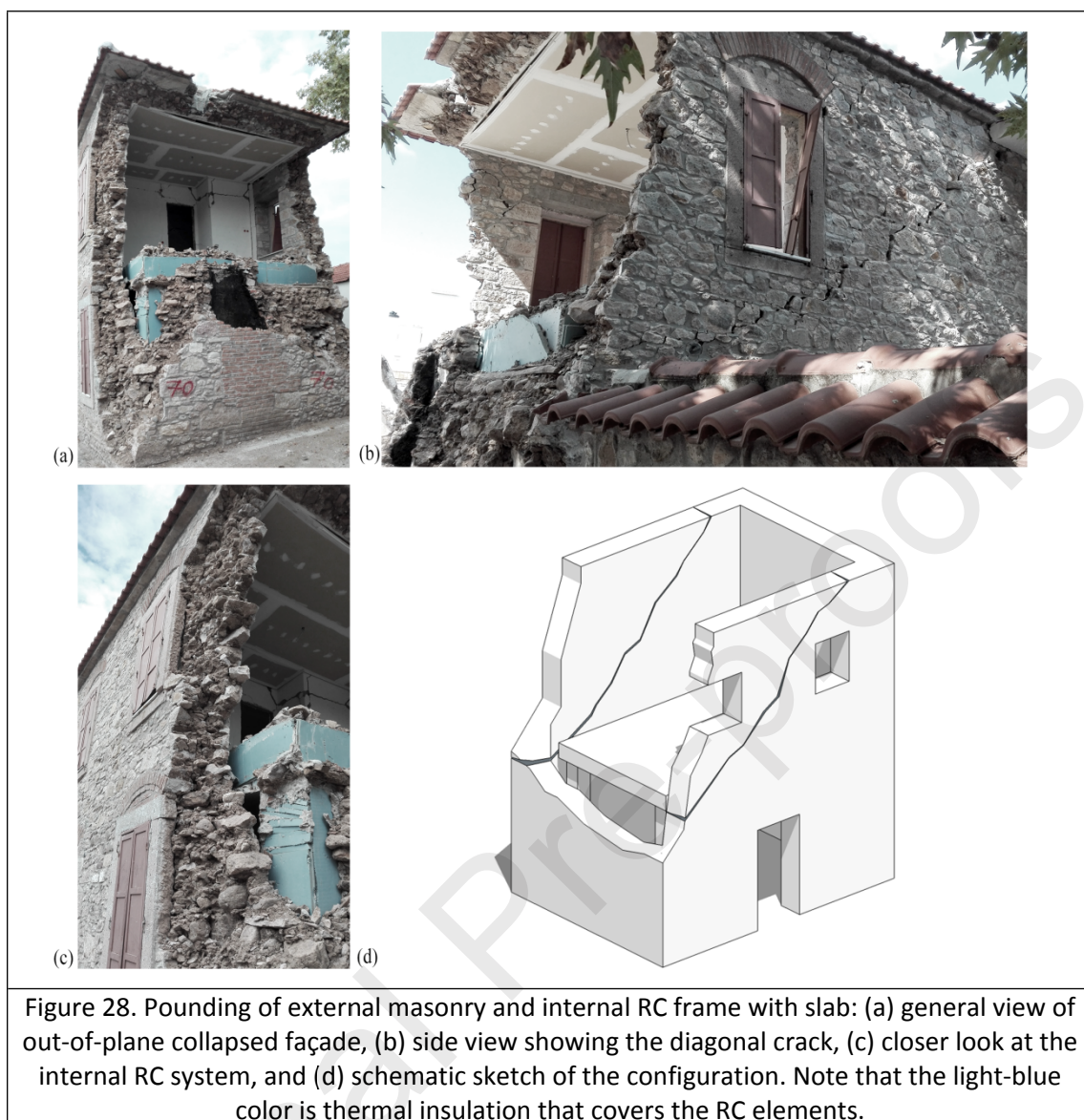


Figure 27. (a)-(b) Buildings strengthened with RC jacketing, which failed due to the poor quality of masonry. (c) Detail of a collapsed masonry portion strengthened with RC jacketing. (d) Schematic sketch of failure of poor masonry strengthened with RC jacketing on one side.

494 4.2 Additions and Alterations

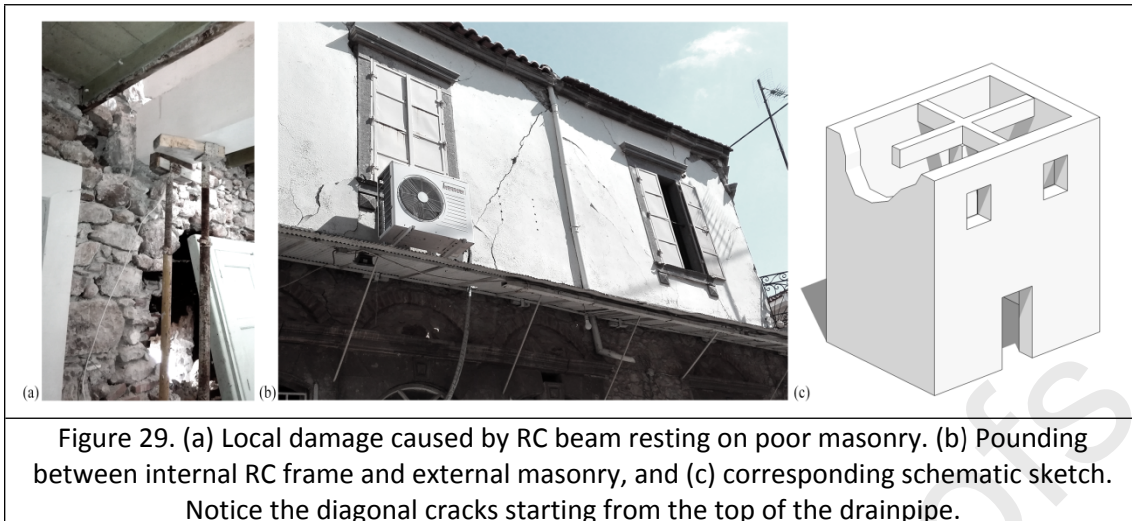
495 Some interventions are not intended to ensure or improve the structural behavior, but are
 496 only realized for functional purposes. A common misunderstanding seems to be present in
 497 such cases: since these interventions do not alter significantly the structural system, an
 498 engineering assessment of the structural unit is not necessary. As a result, some alterations
 499 are badly conceived and might end up being determinant for the structural unit's
 500 performance. Several didactic cases were observed during the field survey.

501 A frequent intervention is the substitution of the timber floors with RC slabs, basically arising
 502 by the easily availability of the material, cost and modern needs of the flooring system. In
 503 order to avoid drastic measures over the existing masonry, some engineers resort to the
 504 solution of adding an internal RC frame separate from the existing structure. The new
 505 internal RC structural system is designed independently of the external existing masonry,
 506 and no connection is enforced. Some cases of this configuration were inspected, among
 507 which one appeared to be catastrophic (Figure 28). Being disconnected, the two structural
 508 systems were characterized by distinct dynamic properties. During the seismic event this
 509 resulted in different displacement demands and at the same time out-of-phase responses,
 510 causing pounding phenomena. The stiff and heavy RC caisson collided with the masonry
 511 walls, inducing severe damage instead of providing strengthening to the existing structure.
 512 In fact, the failure mechanism of the masonry structure observed highlights the behavior, as
 513 the collapsed façade failed under OOP actions exactly at the height of the slab, while the two
 514 transversal walls suffered IP damage that initiated at the aforementioned height and
 515 propagated diagonally, ignoring the openings' layout.



516

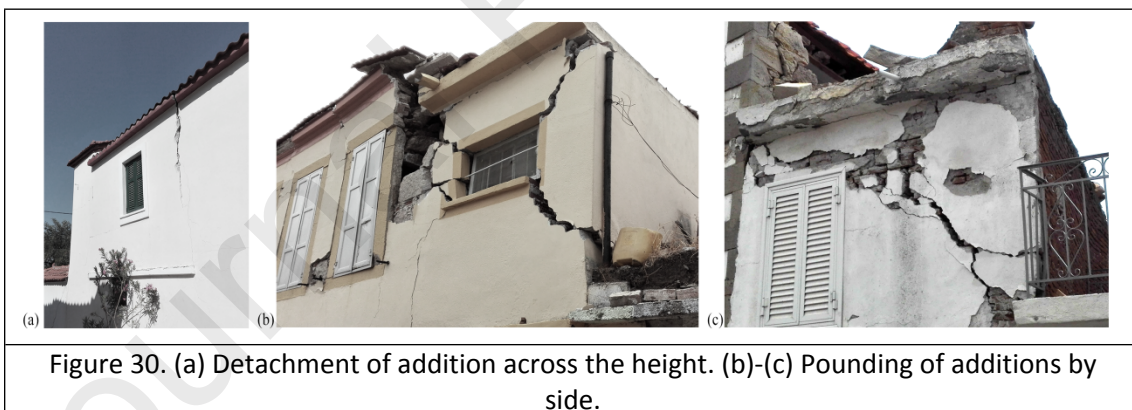
517 A similar intervention scheme inspected included RC columns and beams, the latter resting
 518 on the peripheral masonry façades. In this case, a proper connection among the new RC
 519 beams and the masonry walls was not ensured, resulting into two main damage patterns: 1)
 520 in cases of poor quality of masonry, the concentrated loads caused local disintegration of
 521 masonry (Figure 29 (a)); 2) pounding between masonry and the concrete beams caused
 522 damage to the façades (Figure 29 (b), (c)).



523

524 Interventions that induce irregularities might end up being also decisive for the global
 525 structural integrity. The building shown in Figure 18 (b)-(c) and described in Section 3.2, is a
 526 representative case of this category of interventions with a disastrous outcome.

527 Finally, small additions are also a common intervention practice to increase the housing
 528 space. Additions across the height (in elevation) were observed in some cases to suffer
 529 detachment and potential overturning (Figure 30 (a)). Additions by side (in plan) often acted
 530 beneficially as a buttressing element, constraining the OOP failure. Nevertheless, pounding
 531 between the old masonry and the side addition was also identified (Figure 30 (b), (c)).



532 5. Summary and Conclusions

533 The 2017 Lesvos earthquake induced severe damage to old URM structures at the
 534 southwestern part of the island, and especially in the traditional settlement of Vrissa.
 535 Following previous research that pointed out significant damage in those structures, this
 536 paper discusses the factors that played a role to their performance. To this end, a field
 537 reconnaissance has been conducted in order to record damage and failure patterns, and in
 538 turn draw meaningful conclusions about their response. Particular attention is paid to the
 539 traditional construction techniques and architectural features that appeared to affect the
 540 seismic response of the structures.

541 In general, poor materials were observed as masonry constituents. Combined with the
542 sparse presence of transversal interlocking stones, a significant portion of URM structures
543 appeared to delaminate and disintegrate easily. On the other hand, timber-reinforced
544 masonry structures showed enhanced seismic performance and structural redundancy,
545 suffering only localized damage while avoiding total collapses.

546 Several local mechanisms were inspected and described, i.e. masonry disintegration, gable
547 end wall overturning, corner mechanism and loss of fireplaces' flues embedded in masonry
548 walls. Proper construction details and structural connections could prevent such
549 mechanisms from occurring.

550 Out-of-plane mechanisms were the most frequent, in most cases resulting in partial or even
551 global collapses. The main factors that determined the appearance of such mechanisms
552 could be summarized to be the following: the unconstrained length, the lack of adequate
553 connections with the transversal walls and the horizontal structural elements, the wall
554 slenderness and the presence of plan irregularities. Considering the above, a good
555 configuration of the quoin stones, the presence of dense transversal walls or an entrance
556 recess, and the existence of timber laces or tie rods could decrease the out-of-plane
557 vulnerability. On the contrary, the "utilization" of a pre-existing side wall to make a semi-
558 detached building, the presence of windows or flues in the proximity of the corners and the
559 lack of a horizontal diaphragm were observed to be detrimental for masonry façades.

560 Structures that experienced a box-like behavior presented in-plane response, in generally
561 preferred as it possess a larger capacity to withstand lateral actions. In-plane damage was
562 observed due to weak spandrels and piers, or overweight structures due to RC slabs.

563 Three types of combined in-plane and out-of-plane mechanisms were also reported, scarcely
564 studied in literature. The first two refer to the interaction of in-plane and out-of-plane
565 actions at the corners or recesses of the structure; with the distinguished feature being the
566 presence or absence of constrain at the top. In addition, partial out-of-plane collapses of in-
567 plane damaged walls were also observed.

568 A number of collapses of non-structural elements were also inspected i.e. unconnected
569 posts and lintels, chimney tops, roof tiles, pillars, retaining walls and veneer walls. The
570 collapse of such elements might not affect the global structural stability, yet they could
571 result to important monetary loss and even human fatalities.

572 Finally, an insight of the performance of previous interventions is attempted. Concerning
573 techniques intended to improve the structural behavior; firstly a strengthening prioritization
574 is established, and then some representative non-conforming cases are reported. This way,
575 it is clearly shown that the application of several techniques could be detrimental instead of
576 beneficial if basic conditions are not met. Concerning interventions that are materialized for
577 functional purposes, a number of cases is reported that indicate crucial structural aspects
578 arising. Thus, the importance of engineered and well-conceived alterations in existing
579 buildings is stressed.

580 **Acknowledgements**

581 This work was partly funded by project STAND4HERITAGE that has received funding from the
 582 European Research Council (ERC) under the European Union's Horizon 2020 research and
 583 innovation programme (Grant agreement No. 833123), as an Advanced Grant.

584 The authors would like to thank Maria Kleanthi, Director of the Earthquake Rehabilitation
 585 Organization in Greece, for the assistance in the field reconnaissance campaign; and Dr.
 586 Vasilios G. Bardakis, President of the Greek Association of Civil Engineers, for the support in
 587 writing the first draft.

588 **6. References**

- 589 [1] P. Papadimitriou, I. Kassaras, G. Kaviris, G.A. Tselentis, N. Voulgaris, E. Lekkas, G.
 590 Chouliaras, C. Evangelidis, K. Pavlou, V. Kapetanidis, A. Karakonstantis, D.
 591 Kazantzidou-Firtinidou, I. Fountoulakis, C. Millas, I. Spingos, T. Aspiotis, A.
 592 Moumoulidou, E. Skourtsos, V. Antoniou, E. Andreadakis, S. Mavroulis, M. Kleanthi,
 593 The 12 th June 2017 M w = 6.3 Lesvos earthquake from detailed seismological
 594 observations, *J. Geodyn.* 115 (2018) 23–42.
 595 <https://doi.org/10.1016/j.jog.2018.01.009>.
- 596 [2] National Observatory of Athens, Online ShakeMap Service, Website. (2018).
 597 <https://shake.gein.noa.gr/sm/noa2017lkye/products.html> (accessed March 16,
 598 2020).
- 599 [3] C. Papaioannou, C. Karakostas, M. Rovithis, T. Salonikios, N. Theodoulidis, K. Makra,
 600 V. Lekidis, V. Margaris, K. Morfidis, S. Zacharopoulos, the June-July , 2017 Earthquake
 601 Sequences in Eastern Aegean Sea : Ground Motions , Geotechnical Ground Failures
 602 and Structural Response, in: 16th Eur. Conf. Earthq. Eng., Thessaloniki, Greece, 2018.
- 603 [4] P. Papadimitriou, G.A. Tselentis, N. Voulgaris, V. Kouskouna, E. Lagios, I. Kassaras, G.
 604 Kaviris, K. Pavlou, V. Sakkas, A. Moumoulidou, A. Karakonstantis, V. Kapetanidis, G.
 605 Sakkas, D. Kazantzidou, T. Aspiotis, I. Fountoulakis, C. Millas, I. Spingos, E. Lekkas, V.
 606 Antoniou, S. Mavroulis, E. Skourtsos, E. Andreadakis, Preliminary report on the Lesvos
 607 12 June 2017 Mw=6.3 earthquake, (2017). [https://www.emsc-](https://www.emsc-csem.org/Files/news/Earthquakes_reports/lesvos_report_nkua_v5.pdf)
 608 [csem.org/Files/news/Earthquakes_reports/lesvos_report_nkua_v5.pdf](https://www.emsc-csem.org/Files/news/Earthquakes_reports/lesvos_report_nkua_v5.pdf).
- 609 [5] A. Kiratzi, The 12 June 2017 Mw 6.3 Lesvos Island (Aegean Sea) earthquake: Slip
 610 model and directivity estimated with finite-fault inversion, *Tectonophysics.* 724–725
 611 (2018) 1–10. <https://doi.org/10.1016/j.tecto.2018.01.003>.
- 612 [6] N. Vavlas, A. Kiratzi, V. Margaris, G. Karakaisis, Probabilistic Seismic Hazard
 613 Assessment (PSHA) for Lesvos island using the Logic Tree Approach, *Bull. Geol. Soc.*
 614 *Greece.* 55 (2019) 109–136. <https://doi.org/10.12681/bgsg.20705>.
- 615 [7] K. Chousianitis, A.O. Konca, Coseismic Slip Distribution of the 12 June 2017 Mw = 6.3
 616 Lesvos Earthquake and Imparted Static Stress Changes to the Neighboring Crust, *J.*
 617 *Geophys. Res. Solid Earth.* 123 (2018) 8926–8936.
 618 <https://doi.org/10.1029/2018JB015950>.
- 619 [8] A. Vött, Relative sea level changes and regional tectonic evolution of seven coastal
 620 areas in NW Greece since the mid-Holocene, *Quat. Sci. Rev.* 26 (2007) 894–919.
 621 <https://doi.org/10.1016/j.quascirev.2007.01.004>.

- 622 [9] E. Lekkas, N. Voulgaris, P. Karydis, G.A. Tselentis, E. Skourtsos, V. Antoniou, E.
623 Andreadakis, S. Mavroulis, N. Spirou, F. Speis, P. Papadimitriou, V. Kouskouna, G.
624 Kassaras, G. Kaviris, K. Pavlou, V. Sakkas, G. Chouliaras, Lesvos Earthquake Mw 6.3,
625 June 12, 2017. Preliminary report., Athens, 2017.
- 626 [10] G. Grünthal, R.M.W. Musson, J. Schwartz, M. Stucchi, European Macroseismic Scale
627 1998 (EMS-98), European Seismological Commission, Luxembourg, 1998.
628 [http://lib.riskreductionafrica.org/bitstream/handle/123456789/1193/1281.European](http://lib.riskreductionafrica.org/bitstream/handle/123456789/1193/1281.European%20Macroseismic%20Scale%201998.pdf?sequence=1)
629 [Macroseismic Scale 1998.pdf?sequence=1](http://lib.riskreductionafrica.org/bitstream/handle/123456789/1193/1281.European%20Macroseismic%20Scale%201998.pdf?sequence=1).
- 630 [11] A. Annunziato, G.A. Papadopoulos, A. Yalciner, O. Necmioglu, C. Ozer Sozdinler, A.
631 Agalos, M. Charalampakis, G.G. Dogan, M. Kleanthi, T. Novikova, P. Probst, C. Proietti,
632 I. Triantafyllou, Analysis of the Tsunami Event caused by the Mw 6 . 3 Lesvos Island
633 (East Aegean Sea) Earthquake of 12th June 2017, 2017. [https://www.emsc-](https://www.emsc-csem.org/Doc/Additional_Earthquake_Report/597714/Analysis_of_the_Tsunami_Event_caused_by_the_Mw_6.3_Plomari_Earthquake_of_12_June_2017_v2.1.pdf%0D)
634 [csem.org/Doc/Additional_Earthquake_Report/597714/Analysis of the Tsunami Event](https://www.emsc-csem.org/Doc/Additional_Earthquake_Report/597714/Analysis_of_the_Tsunami_Event_caused_by_the_Mw_6.3_Plomari_Earthquake_of_12_June_2017_v2.1.pdf%0D)
635 [caused by the Mw 6.3 Plomari Earthquake of 12 June 2017. v2.1.pdf%0D](https://www.emsc-csem.org/Doc/Additional_Earthquake_Report/597714/Analysis_of_the_Tsunami_Event_caused_by_the_Mw_6.3_Plomari_Earthquake_of_12_June_2017_v2.1.pdf%0D).
- 636 [12] S. Mavroulis, E. Andreadakis, N.I. Spyrou, V. Antoniou, E. Skourtsos, P. Papadimitriou,
637 I. Kassaras, G. Kaviris, G.A. Tselentis, N. Voulgaris, P. Carydis, E. Lekkas, UAV and GIS
638 based rapid earthquake-induced building damage assessment and methodology for
639 EMS-98 isoseismal map drawing: The June 12, 2017 Mw 6.3 Lesvos (Northeastern
640 Aegean, Greece) earthquake, *Int. J. Disaster Risk Reduct.* 37 (2019) 101169.
641 <https://doi.org/10.1016/j.ijdr.2019.101169>.
- 642 [13] N. Chatzis, C. Kkallas, C. Papazachos, M. Anthymidis, E. Rovithis, C. Karakostas, C.
643 Papaioannou, Stochastic Simulation of Seismic Motion and Site-Effects Studies of
644 Ambient Noise and Seismic Data : The Case of the Vriza Settlement and the 2017 M =
645 6 . 3 Lesvos Earthquake, (2019) 24–25.
646 <https://doi.org/10.1029/2009GL038863.Motazedian>.
- 647 [14] J. Hecht, Geological map of Greece,1:50.000. Plomari-Mytilene, Ayia Paraskevi,
648 Mithimna, Polichnitos and Eressos sheets., *Inst. Geol. Miner. Explor. Greece.* (1972).
- 649 [15] M. Bruneau, State-of-the-art report on seismic performance of unreinforced masonry
650 buildings, *J. Struct. Eng. (United States)*. 120 (1994) 230–251.
651 [https://doi.org/10.1061/\(ASCE\)0733-9445\(1994\)120:1\(230\)](https://doi.org/10.1061/(ASCE)0733-9445(1994)120:1(230)).
- 652 [16] D. Penazzi, M.R. Valluzzi, G. Cardani, L. Binda, G. Baronio, C. Modena, C., Behaviour of
653 Historic Masonry Buildings in Seismic Areas: Lessons Learned from the Umbria-
654 Marche Earthquake, 12th Int. Brick/Block Mason. Conf. Madrid, Spain. (2000) 217–
655 235.
- 656 [17] D. Gautam, H. Rodrigues, K.K. Bhetwal, P. Neupane, Y. Sanada, Common structural
657 and construction deficiencies of Nepalese buildings, *Innov. Infrastruct. Solut.* 1 (2016)
658 1–18. <https://doi.org/10.1007/s41062-016-0001-3>.
- 659 [18] M. Shakya, C.K. Kawan, Reconnaissance based damage survey of buildings in
660 Kathmandu valley: An aftermath of 7.8Mw, 25 April 2015 Gorkha (Nepal) earthquake,
661 *Eng. Fail. Anal.* 59 (2016) 161–184.
662 <https://doi.org/10.1016/j.engfailanal.2015.10.003>.
- 663 [19] L. Decanini, A. De Sortis, A. Goretti, R. Langenbach, F. Mollaioli, A. Rasulo,
664 Performance of masonry buildings during the 2002 Molise, Italy, earthquake, *Earthq.*
665 *Spectra.* 20 (2004) 191–220. <https://doi.org/10.1193/1.1765106>.

- 666 [20] F. Aras, E. Düzci, Seismic Performance of Traditional Stone Masonry Dwellings under
667 Çanakkale Seismic Sequences, *J. Perform. Constr. Facil.* 32 (2018) 1–11.
668 [https://doi.org/10.1061/\(ASCE\)CF.1943-5509.0001173](https://doi.org/10.1061/(ASCE)CF.1943-5509.0001173).
- 669 [21] L. Sorrentino, S. Cattari, F. da Porto, G. Magenes, A. Penna, Seismic behaviour of
670 ordinary masonry buildings during the 2016 central Italy earthquakes, *Bull. Earthq.
671 Eng.* 17 (2019) 5583–5607. <https://doi.org/10.1007/s10518-018-0370-4>.
- 672 [22] M. Javed, A.N. Khan, A. Penna, G. Magenes, Behaviour of Masonry Structures During
673 the Kashmir 2005, in: *First Eur. Conf. Earthq. Eng. Seismol.*, Geneva, 2006.
- 674 [23] E. Vintzileou, A. Zagkotsis, C. Repapis, C. Zeris, Seismic behaviour of the historical
675 structural system of the island of Lefkada, Greece, *Constr. Build. Mater.* 21 (2007)
676 225–236. <https://doi.org/10.1016/j.conbuildmat.2005.04.002>.
- 677 [24] A. Naseer, A. Naeem Khan, Z. Hussain, Q. Ali, Observed seismic behavior of buildings
678 in Northern Pakistan during the 2005 Kashmir earthquake, *Earthq. Spectra.* 26 (2010)
679 425–449. <https://doi.org/10.1193/1.3383119>.
- 680 [25] N. Augenti, F. Parisi, Learning from construction failures due to the 2009 L'Aquila,
681 Italy, earthquake, *J. Perform. Constr. Facil.* 24 (2010) 536–555.
682 [https://doi.org/10.1061/\(ASCE\)CF.1943-5509.0000122](https://doi.org/10.1061/(ASCE)CF.1943-5509.0000122).
- 683 [26] M. Indirli, L.A.S. Kouris, A. Formisano, R.P. Borg, F.M. Mazzolani, Seismic damage
684 assessment of unreinforced masonry structures after the Abruzzo 2009 earthquake:
685 The case study of the historical centers of L'Aquila and Castelvechio Subequo, *Int. J.
686 Archit. Herit.* 7 (2013) 536–578. <https://doi.org/10.1080/15583058.2011.654050>.
- 687 [27] D. Dizhur, J. Ingham, L. Moon, M. Griffith, A. Schultz, I. Senaldi, G. Magenes, J. Dickie,
688 S. Lissel, J. Centeno, C. Ventura, J. Leite, P. Lourenco, Performance of masonry
689 buildings and churches in the 22 February 2011 Christchurch earthquake, *Bull. New
690 Zeal. Soc. Earthq. Eng.* 44 (2011) 279–296. <https://doi.org/10.5459/bnzsee.44.4.279-296>.
- 692 [28] G.P. Cimellaro, I.P. Christovasilis, A.M. Reinhorn, A. De Stefano, T. Kirova, L'Aquila
693 Earthquake of April 6, 2009 in Italy: Rebuilding a Resilient City To Withstand Multiple
694 Hazards, 2010.
- 695 [29] J. Ingham, M. Griffith, Performance of unreinforced masonry buildings during the
696 2010 darfi eld (Christchurch, NZ) earthquake, *Aust. J. Struct. Eng.* 11 (2011) 207–224.
697 <https://doi.org/10.1080/13287982.2010.11465067>.
- 698 [30] L. Moon, D. Dizhur, I. Senaldi, H. Derakhshan, M. Griffith, G. Magenes, J. Ingham, The
699 demise of the URM building stock in Christchurch during the 2010–2011 Canterbury
700 earthquake sequence, *Earthq. Spectra.* 30 (2014) 253–276.
701 <https://doi.org/10.1193/022113EQS044M>.
- 702 [31] I. Senaldi, G. Magenes, J.M. Ingham, Damage Assessment of Unreinforced Stone
703 Masonry Buildings After the 2010–2011 Canterbury Earthquakes, *Int. J. Archit. Herit.* 9
704 (2015) 605–627. <https://doi.org/10.1080/15583058.2013.840688>.
- 705 [32] Z. Celep, A. Erken, B. Taskin, A. Ilki, Failures of masonry and concrete buildings during
706 the March 8, 2010 Kovancilar and Palu (Elazığ) Earthquakes in Turkey, *Eng. Fail. Anal.*
707 18 (2011) 868–889. <https://doi.org/10.1016/j.engfailanal.2010.11.001>.

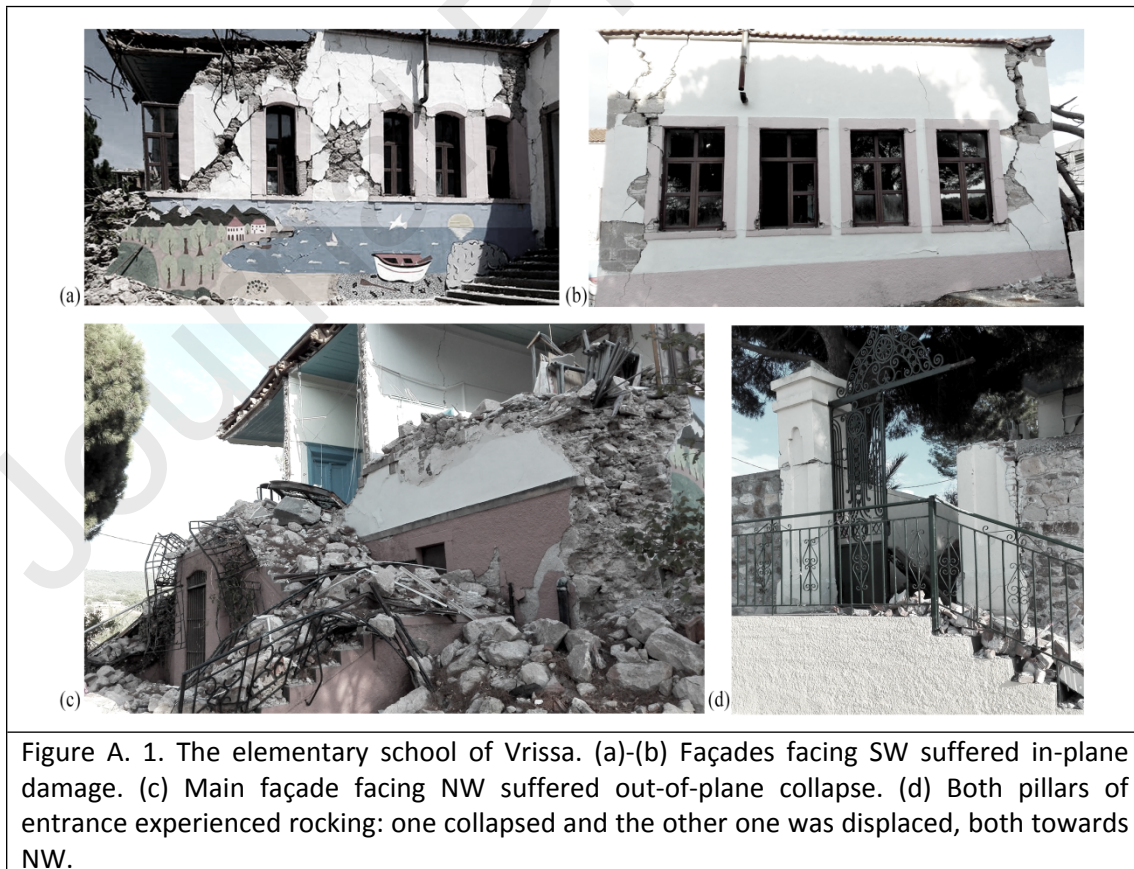
- 708 [33] A. Penna, P. Morandi, M. Rota, C.F. Manzini, F. da Porto, G. Magenes, Performance of
709 masonry buildings during the Emilia 2012 earthquake, *Bull. Earthq. Eng.* 12 (2014)
710 2255–2273. <https://doi.org/10.1007/s10518-013-9496-6>.
- 711 [34] L. Sorrentino, L. Liberatore, D. Liberatore, R. Masiani, The behaviour of vernacular
712 buildings in the 2012 Emilia earthquakes, *Bull. Earthq. Eng.* 12 (2014) 2367–2382.
713 <https://doi.org/10.1007/s10518-013-9455-2>.
- 714 [35] E. Sayin, B. Yön, Y. Calayir, M. Karaton, Failures of masonry and adobe buildings
715 during the June 23, 2011 Maden-(Elazığ) earthquake in Turkey, *Eng. Fail. Anal.* 34
716 (2013) 779–791. <https://doi.org/10.1016/j.engfailanal.2012.10.016>.
- 717 [36] D. Dizhur, R.P. Dhakal, J. Bothara, J.M. Ingham, Building typologies and failure modes
718 observed in the 2015 Gorkha (Nepal) earthquake, *Bull. New Zeal. Soc. Earthq. Eng.* 49
719 (2016) 211–232. <https://doi.org/10.5459/bnzsee.49.2.211-232>.
- 720 [37] R. Sisti, M. Di Ludovico, A. Borri, A. Prota, Damage assessment and the effectiveness
721 of prevention: the response of ordinary unreinforced masonry buildings in Norcia
722 during the Central Italy 2016–2017 seismic sequence, *Bull. Earthq. Eng.* 17 (2019)
723 5609–5629. <https://doi.org/10.1007/s10518-018-0448-z>.
- 724 [38] N. Ambraseys, *Earthquakes in the Eastern Mediterranean and the Middle East, A*
725 *Multidisciplinary Study of Seismicity up to 1900*, Cambridge, 2009.
- 726 [39] D. Mirabile Gattia, G. Roselli, O. Alshawa, P. Cinaglia, G. Di Girolami, C. Francola, F.
727 Persia, E. Petrucci, R. Piloni, F. Scognamiglio, L. Sorrentino, S. Zamponi, D. Liberatore,
728 Characterization of historical masonry mortar from sites damaged during the central
729 Italy 2016-2017 seismic sequence: The case study of Arquata del Tronto, *Ann.*
730 *Geophys.* 62 (2019). <https://doi.org/10.4401/ag-8019>.
- 731 [40] O. Alshawa, D. Liberatore, L. Sorrentino, Dynamic One-Sided Out-Of-Plane Behavior
732 of Unreinforced-Masonry Wall Restrained by Elasto-Plastic Tie-Rods, *Int. J. Archit.*
733 *Herit.* 13 (2019) 340–357. <https://doi.org/10.1080/15583058.2018.1563226>.
- 734 [41] E. Vintzileou, Timber-reinforced structures in Greece: 2500 BC-1900 AD, *Proc. Inst.*
735 *Civ. Eng. Struct. Build.* 164 (2011) 167–180. <https://doi.org/10.1680/stbu.9.00085>.
- 736 [42] A. Tavares, D. D’Ayala, A. Costa, H. Varum, Construction systems, in: A. Costa, J.M.
737 Guedes, H. Varum (Eds.), *Struct. Rehabil. Old Build., Building P*, Springer Heidelberg
738 New York Dordrecht London Library, 2014: pp. 1–35. <https://doi.org/10.1007/978-3-642-39686-1>.
- 740 [43] N. Ruggieri, G. Tampone, R. Zinno, *Historical Earthquake-Resistant Timber Frames in*
741 *the Mediterranean Area*, Springer Heidelberg New York Dordrecht London, 2015.
742 <https://doi.org/10.1007/978-3-319-16187-7>.
- 743 [44] J. Ortega, G. Vasconcelos, H. Rodrigues, M. Correia, P.B. Lourenço, Traditional
744 earthquake resistant techniques for vernacular architecture and local seismic
745 cultures: A literature review, *J. Cult. Herit.* 27 (2017) 181–196.
746 <https://doi.org/10.1016/j.culher.2017.02.015>.
- 747 [45] N. Karydis, Traditional Earthquake-resistant Construction in the East Aegean Sea: The
748 Case of Eresos and Pergamon [in Greek], in: *3rd Natl. Conf. Earthq. Eng. Eng. Seismol.*,
749 Athens, 2008.

- 750 [46] R. Langenbach, From “Opus Craticium” to the “Chicago frame”: Earthquake-resistant
751 traditional construction, *Int. J. Archit. Herit.* 1 (2007) 29–59.
752 <https://doi.org/10.1080/15583050601125998>.
- 753 [47] T. Makarios, M. Demosthenous, Seismic response of traditional buildings of Lefkas
754 Island, Greece, *Eng. Struct.* 28 (2006) 264–278.
755 <https://doi.org/10.1016/j.engstruct.2005.08.002>.
- 756 [48] C. Casapulla, A. Maione, Experimental and Analytical Investigation on the Corner
757 Failure in Masonry Buildings: Interaction between Rocking-Sliding and Horizontal
758 Flexure, *Int. J. Archit. Herit.* 14 (2020) 208–220.
759 <https://doi.org/10.1080/15583058.2018.1529206>.
- 760 [49] L. Giresini, F. Solarino, O. Paganelli, D. V. Oliveira, M. Froli, ONE-SIDED rocking
761 analysis of corner mechanisms in masonry structures: Influence of geometry, energy
762 dissipation, boundary conditions, *Soil Dyn. Earthq. Eng.* 123 (2019) 357–370.
763 <https://doi.org/10.1016/j.soildyn.2019.05.012>.
- 764 [50] Google, Google Maps, (n.d.).
765 https://www.google.com/maps/@39.0410673,26.2011979,3a,75y,189.01h,95.33t/data=!3m6!1e1!3m4!1shyrhi_AjyrUW-hIEyocZlQ!2e0!7i13312!8i6656 (accessed March
766 22, 2020).
767
- 768 [51] D. Perrone, P.M. Calvi, R. Nascimbene, E.C. Fischer, G. Magliulo, Seismic performance
769 of non-structural elements during the 2016 Central Italy earthquake, *Bull. Earthq.
770 Eng.* 17 (2019) 5655–5677. <https://doi.org/10.1007/s10518-018-0361-5>.
- 771 [52] L. Binda, A. Saisi, C. Tedeschi, Compatibility of materials used for repair of masonry
772 buildings: research and applications, 2006. [https://doi.org/10.1007/978-1-4020-
773 5077-0_11](https://doi.org/10.1007/978-1-4020-5077-0_11).
- 774 [53] C. Modena, M.R. Valluzzi, F. da Porto, F. Casarin, M. Munari, N. Mazzon, M. Panizza,
775 Assessment and improvement of the seismic safety of historic constructions:
776 research and applications in Italy, in: *I Congr. Iberoam. Sobre Construcciones
777 Históricas y Estructuras Mampostería*, 2008.
- 778 [54] C. Modena, M.R. Valluzzi, F. Da Porto, F. Casarin, Structural aspects of the
779 conservation of historic masonry constructions in seismic areas: Remedial measures
780 and emergency actions, *Int. J. Archit. Herit.* 5 (2011) 539–558.
781 <https://doi.org/10.1080/15583058.2011.569632>.
- 782 [55] D. Dizhur, N. Ismail, C. Knox, R. Lumantarna, J.M. Ingham, Performance of
783 unreinforced and retrofitted masonry buildings during the 2010 darfield earthquake,
784 *Bull. New Zeal. Soc. Earthq. Eng.* 43 (2010) 321–339.
785 <https://doi.org/10.5459/bnzsee.43.4.321-339>.
- 786 [56] G. Correia Lopes, R. Vicente, T.M. Ferreira, M. Azenha, Intervened URM buildings
787 with RC elements: typological characterisation and associated challenges, Springer
788 Netherlands, 2019. <https://doi.org/10.1007/s10518-019-00651-y>.

789 7. Appendix A – Structural Observations on Seismic Motion 790 Directivity

791 According to [5], [7] and [1] among others, the rupture of the seismic event propagated
792 unilaterally towards NW, causing a forward directivity of the seismic motion. This section
793 attempts to shed light to the seismic motion directivity through structural observations. Two
794 cases are presented, whose damage and failure pattern can reveal the main seismic
795 component. Inherent uncertainties and limitations exist in this attempt, some of which are
796 pointed out; yet the observations appear profound not to be mentioned.

797 The first case concerns the elementary school of the Vrissa settlement (Figure A. 1). Figure A.
798 1 (a)-(b) presents two façades that are facing SW and suffered IP damage. Figure A. 1 (c)
799 illustrates the main façade of the school that faces NW and suffered complete OOP collapse.
800 Moreover, Figure A. 1 (d) depicts the main entrance of the school that faces NW and is
801 composed by two pillars. Both pillars experienced rocking at the height of the side retaining
802 walls; with the one on the right collapsing outwards (towards NW) and the one on the left
803 being displaced of about 5 cm at this height, towards NW. All the above observations point
804 out a seismic motion directivity towards NW. Nevertheless, let us make some more notes
805 about the building. It is constructed on a hill at the SW of the settlement, with slopes in all
806 the surrounding, except SE. Thus slope movement might affected the severity in some
807 direction. In fact, a local landslide occurred at the NE side and the corresponding façade (not
808 showed herein) collapsed OOP. Nevertheless, all the rest façades and the pillars of the
809 entrance point out the same seismic motion directivity towards NW.



811 Finally, the second case concerns the building presented in Section 4.2 and Figure 28. The
812 observations made there indicate that pounding occurred between the internal RC frame
813 and slab with the external masonry façade. By looking at the damage pattern it is clear that
814 the collision happened at the interface between the slab and the façade that collapsed OOP,
815 while the transversal façades showed only IP damage induced by the previous collision. The
816 façade that collapsed faces SE, while the two transversal façades face SW and NE. Since
817 pounding occurs at large displacements, the aforementioned damage pattern points out
818 that the main seismic component was in the NW-SE direction.